

NAVAL POSTGRADUATE SCHOOL MONTEREY, CALIFORNIA



THESIS

**DETECTION AND TARGET-STRENGTH MEASUREMENTS OF
BURIED OBJECTS USING A SEISMO-ACOUSTIC SONAR**

by

Patrick W. Hall

December 1998

Thesis Advisors:

Thomas G. Muir
Steven R. Baker

19990120 077

Approved for public release; distribution is unlimited.

REPORT DOCUMENTATION PAGE			Form Approved OMB No. 0704-0188	
Public reporting burden for this collection of information is estimated to average 1 hour per response, including the time for reviewing instruction, searching existing data sources, gathering and maintaining the data needed, and completing and reviewing the collection of information. Send comments regarding this burden estimate or any other aspect of this collection of information, including suggestions for reducing this burden, to Washington Headquarters Services, Directorate for Information Operations and Reports, 1215 Jefferson Davis Highway, Suite 1204, Arlington, VA 22202-4302, and to the Office of Management and Budget, Paperwork Reduction Project (0704-0188) Washington DC 20503.				
1. AGENCY USE ONLY (Leave blank)		2. REPORT DATE December 1998		3. REPORT TYPE AND DATES COVERED Master's Thesis
4. TITLE AND SUBTITLE DETECTION AND TARGET-STRENGTH MEASUREMENTS OF BURIED OBJECTS USING A SEISMO-ACOUSTIC SONAR			5. FUNDING NUMBERS	
6. AUTHOR(S) Patrick W. Hall				
7. PERFORMING ORGANIZATION NAME(S) AND ADDRESS(ES) Naval Postgraduate School Monterey CA 93943-5000			8. PERFORMING ORGANIZATION REPORT NUMBER	
9. SPONSORING/MONITORING AGENCY NAME(S) AND ADDRESS(ES)			10. SPONSORING/MONITORING AGENCY REPORT NUMBER	
11. SUPPLEMENTARY NOTES The views expressed in this thesis are those of the author and do not reflect the official policy or position of the Department of Defense or the U.S. Government.				
12a. DISTRIBUTION/AVAILABILITY STATEMENT Approved for public release; distribution is unlimited.			12b. DISTRIBUTION CODE	
13. ABSTRACT (maximum 200 words) This thesis describes the results of field experiments in which seismo-acoustic interface (Rayleigh) waves were employed to detect and measure the target strength of mine-like test objects buried in the near-surf zone. These experiments were conducted as part of an ongoing NPS research program to develop a seismo-acoustic sonar system for the detection of buried mines in the surf and near-surf zones. An experimental seismo-acoustic sonar system, using linear force actuators as the wave source and three-axis seismometers as receivers, was deployed at a beach test site. The target strengths of two mine-like test objects, a compressed gas cylinder and a gunpowder can, were measured as a function of target mass and for various emplacement conditions, e.g. very wet sand, not very wet sand, partially buried, completely buried, completely buried and washed over for several days. "Vector polarization filtering" was employed to separate the reflected signal due to Rayleigh waves, for which the particle motion is elliptical, from that of body (P and S) waves, for which the particle motion is linear. The target strength was generally found to increase with increasing target mass. Typical values observed ranged from approximately -20 dB to -10 dB for target masses of 70 to 290 kg. Curiously, it was observed that the elliptical particle motion of the reflected wave was of the opposite polarity for those targets which were buried, but slightly exposed, compared to those which were completely buried. It is not known at this time whether this is due to the depth-dependent properties of Rayleigh waves, or whether it is a result of the conditions of source and target emplacement.				
14. SUBJECT TERMS Seismo-Acoustic Sonar, surface waves, buried object detection, mine detection			15. NUMBER OF PAGES 74	
			16. PRICE CODE	
17. SECURITY CLASSIFICATION OF REPORT Unclassified	18. SECURITY CLASSIFICATION OF THIS PAGE Unclassified	19. SECURITY CLASSIFICATION OF ABSTRACT Unclassified	20. LIMITATION OF ABSTRACT UL	

NSN 7540-01-280-5500

Standard Form 298 (Rev. 2-89)
Prescribed by ANSI Std. Z39-18 298-102

(This page intentionally blank)

Approved for public release; distribution is unlimited.

**DETECTION AND TARGET-STRENGTH MEASUREMENTS OF
BURIED OBJECTS USING A SEISMO-ACOUSTIC SONAR**

Patrick W. Hall

Major, United States Marine Corps

BS, United States Naval Academy, 1986

Submitted in partial fulfillment
of the requirements for the degree of

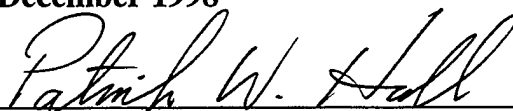
MASTER OF SCIENCE IN APPLIED PHYSICS

from the

NAVAL POSTGRADUATE SCHOOL

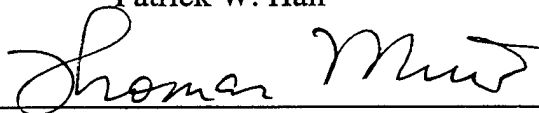
December 1998

Author:



Patrick W. Hall

Approved by:



Thomas G. Muir, Thesis Advisor



Steven R. Baker, Thesis Advisor



William B. Maier, Chairman

Department of Physics

(This page intentionally blank)

ABSTRACT

This thesis describes the results of field experiments in which seismo-acoustic interface (Rayleigh) waves were employed to detect and measure the target strength of mine-like test objects buried in the near-surf zone. These experiments were conducted as part of an ongoing NPS research program to develop a seismo-acoustic sonar system for the detection of buried mines in the surf and near-surf zones. An experimental seismo-acoustic sonar system, using linear force actuators as the wave source and three-axis seismometers as receivers, was deployed at a beach test site. The target strengths of two mine-like test objects, a compressed gas cylinder and a gunpowder can, were measured as a function of target mass and for various emplacement conditions, e.g. very wet sand, not very wet sand, partially buried, completely buried, completely buried and washed over for several days. "Vector polarization filtering" was employed to separate the reflected signal due to Rayleigh waves, for which the particle motion is elliptical, from that of body (P and S) waves, for which the particle motion is linear. The target strength was generally found to increase with increasing target mass. Typical values observed ranged from approximately -20 dB to -10 dB for target masses of 70 to 290 kg. Curiously, it was observed that the elliptical particle motion of the reflected wave was of the opposite polarity for those targets which were buried, but slightly exposed, compared to those which were completely buried. It is not known at this time whether this is due to the depth-dependent properties of Rayleigh waves, or whether it is a result of the conditions of source and target emplacement.

(This page intentionally blank)

TABLE OF CONTENTS

I. INTRODUCTION.....	1
A. IMPORTANCE OF RESEARCH	2
B. MILITARY RELEVANCE	4
1. Current MCM Techniques and Technologies.....	5
a. Water Mine Warfare Technologies	5
b. Land Warfare Mine Countermeasures	6
2. Emerging MCM Techniques and Technologies	7
C. OBJECTIVE OF RESEARCH	8
1. Background Subtraction.....	9
2. Low Target Return Strengths.....	10
3. Vector Polarization Filtering.....	10
4. Summary	11
II. PREVIOUS RESEARCH AND DEVELOPMENT	13
A. RESEARCH AT NPS	13
1. Buried Object Detection	13
2. Discrete-Mode Source Development.....	15
B. RESEARCH AT ARL-UT.....	17
C. UNDERWATER EXPERIMENTS USING SONAR.....	19
D. CURRENT RESEARCH AT NPS	19
III. RESEARCH METHODOLOGY	21
A. SOURCE DEVELOPMENT	21
B. DATA COLLECTION EQUIPMENT	23
C. GENERAL EXPERIMENT INFORMATION.....	25
1. Research Site Characterization	25
2. Targets.....	27

3. Preliminary Procedures	30
a. Determination of Optimum Propagation Frequency	31
b. Determination of Surface Wave Speed	31
D. SIGNAL PROCESSING METHODS AND TARGET DETECTION	
EXPERIMENTS	32
1. Signal Processing Methods	32
a. Source Signal Generation and Processing	33
b. Received Signal Processing	33
c. Signal Analysis	34
2. Target Detection Experiments	36
3. Summary	39
IV. TARGET DETECTION AND TARGET-STRENGTH MEASUREMENTS	41
A. CALCULATIONS OF TARGET STRENGTHS	41
B. TARGET DETECTIONS AND TARGET-STRENGTH MEASUREMENTS	44
1. Empty Gas Cylinder, October 16th 1998	45
2. Empty Gas Cylinder, October 20th 1998	46
3. Gas Cylinder, October 23rd 1998	47
4. Gas Cylinder, November 6th 1998	49
5. Powder Keg, November 10th 1998	51
C. OBSERVATIONS AND SUMMARY	53
V. CONCLUSIONS	57
LIST OF REFERENCES	59
INITIAL DISTRIBUTION LIST	61

ACKNOWLEDGMENT

The author would like to acknowledge the financial support of Dr. Douglas Todoroff, Office of Naval Research, Code 321. This work was performed under Research Project No. 03201.

A thanks also goes to George Jaksha and Gary Beck of the NPS Physics Department Machine Shop. Without their timely advice, motivation, and willingness to do whatever was necessary whenever asked, this thesis work may not have progressed as far as it did.

The author would also like to thank Professors Muir and Baker for their guidance and freedom to work and experiment during the course of this thesis work. And finally, I would like to thank my wife, Stephanie, whose willingness to give up countless hours together in order to complete this thesis, contributed greatly to its eventual success.

(This page intentionally blank)

I. INTRODUCTION

This thesis presents experimental results from research work conducted during the development and implementation of a seismo-acoustic sonar system. The purpose of this system is expressly to detect buried objects, principally in the beach, surf zone, and near-shore environments. Here the sediments dominate the acoustical physics. Because sediment structures are elastic, a number of vector wave types arise that are not important in conventional underwater sound, but some waves are excited that possess very useful characteristics. These include a large family of seismo-acoustic waves, which can be generated through surface or bottom interaction and then go on to propagate, reflect, refract, and become involved with interfaces and sedimentary layers. Seismo-acoustic waves are so called because their velocities depend on both the compressional (P) and shear (S) moduli. Of potential practical interest are the seismo-acoustic interface waves that travel along boundaries between media. The utilization of these unique characteristics of seismic waves, specifically surface, or interface, waves, provide the most promise for the detection of shallow buried objects. Interface waves, Rayleigh and Scholte, which propagate at the beach sediment-air and seafloor-water interfaces, respectively, can be used to detect and localize buried objects in those environments. [Ref. 1]

Theoretically, the vector properties of Rayleigh and Scholte interface waves pertain to the case of a homogeneous, isotropic, elastic halfspace overlain by a vacuum or water, respectively. Interface waves are characterized by:

- Propagation along the interface with exponentially decaying amplitude away from the interface in both media.
- Elliptical particle motion in the vertical plane with retrograde orbit just beneath the surface, changing to prograde within a small fraction of a wavelength in depth.
- Continuity of the vertical particle velocity at the interface.
- Discontinuity of the horizontal particle velocity at the interface, building up to a maximum amplitude at a larger fraction of a wavelength in depth.

- No low frequency cutoff.
- A propagation speed and attenuation very close to the bulk shear properties of the medium. [Ref. 1]

Specific to this research is the detection and target-strength measurements of buried objects in the beach and surf zone locales. Realistically, these objects would consist of land and naval military mines placed or buried in the shore environment. For the purposes of this research, the scattering of seismo-acoustic interface waves from several mine-like objects, bearing relative characteristics similar to actual mines, are investigated. This research, sponsored by the Office of Naval Research (ONR), follows previous research efforts conducted by the Applied Research Laboratory at the University of Texas at Austin (ARL-UT) [Ref. 2 & 3] and the work at the Naval Postgraduate School (NPS) in Monterey, California [Ref. 4].

A. IMPORTANCE OF RESEARCH

Mine warfare and the resulting mine countermeasures effort to combat mines have been an integral part of warfighting since the American Revolutionary War, becoming quite effective in the United States Civil War. The use of mines to blockade ports and waterways or to deny access to various bodies of water has been prevalent in every major conflict of the 20th Century. In World War I, the use of mines to deny German submarines access to British coastal waters contributed to the winning effort on the European continent. The use of extensive minefields placed a virtual stranglehold on Japan's naval commerce during World War II, essentially isolating the island nation from its resources. In Korea, Vietnam, and the Persian Gulf War, naval mines have been utilized effectively to harass, disrupt, and prevent both naval and amphibious operations. The presence of mines in Wonsan Harbor in Korea, Haiphong Harbor in North Vietnam, and their use throughout the Persian Gulf played a pivotal role in each of those conflicts. Perhaps the most significant use of naval mines were those used by Iraq against coalition forces during the Gulf War, resulting in extensive damage to the USS Tripoli (LPH-10)

and the USS Princeton (CG-59) and further restricting naval operations in that area. However, sea mines are not the only hurdle facing naval and amphibious forces. [Ref. 6]

Land mines have added a complex and often perplexing dimension to operations ashore. The introduction and widespread use of land mines during World War I ushered in a new warfare concept. The use of land mines, millions of them, in dense belts interlaced among equally dense obstacle belts, was used extensively throughout that war. The continued use of land mines in subsequent conflicts, to include World War II, Korea, Vietnam, and the Gulf War, continually reinforced their role as a force multiplier by inflicting casualties, destroying equipment and material, and denying opposing forces access and freedom-of-movement. The concept of land mines, and also naval mines, as an inexpensive, reliable, low-maintenance, emplace-and-forget weapons system is one easily grasped and continually exploited. Both government and opposition forces have indiscriminately sown millions of land mines in strife-torn countries around the world. In 1994, an estimated 110 million land mines lie active in 64 different countries [Ref. 5]. More than 48 countries are known to have mine-laying capabilities and access to mine inventories. Approximately 30 countries are actively engaged in development and manufacture of new mines and over 20 countries are known exporters of mines. Any country can rapidly acquire and use land and naval mines; it simply requires money to buy them and personnel to emplace them. [Ref. 6]

With the widespread use of mines prevalent in the various unstable regions of the world, measures to counter this threat remain a challenge for U.S. forces. Their appearance in all spectra of warfare, conventional warfare in Kuwait, humanitarian relief in Somalia, peacekeeping in Bosnia, truce compliance on the Korean Peninsula, and border defense in Cuba, require that the U.S. possess robust and capable mine countermeasure systems. These systems must be able to detect, localize, classify, and eventually clear and dispose of mines. The shifting of the naval service's focus from an open-ocean warfighting strategy to one involving the littoral regions of the world has reinforced the emergence of mine warfare as an essential capability. With the use of mines expected to only increase in the near future, the U.S. must pursue technologies that provide the warfighter the ability to quickly, economically, and efficiently defeat the threat.

B. MILITARY RELEVANCE

The end of the Cold War has brought about a redirection of the naval service's warfighting efforts. Previously oriented toward a Soviet foe in an open-ocean conflict, naval forces are now required to maneuver from the sea into the littorals. *Joint Vision 2010* calls for the forward presence and engagement of U.S. forces. To support that idea, the Navy and Marine Corps have developed two concepts; *Forward...From The Sea* (FFTS) and *Operational Maneuver From The Sea* (OMFTS). Both envision the projection of combat power ashore by using the sea as maneuver space. Another supporting idea is *Ship To Objective Maneuver* (STOW). STOW consists of assault forces moving directly and rapidly to inland objectives, foregoing any build-up of support elements ashore, and instead relying on sea-based logistics. The standing requirement for effective mine countermeasures (MCM), employed in the littoral areas to facilitate operations, cannot be understated. Naval and amphibious forces must have an effective MCM capability to operate in distant waters in the early stages of regional hostilities, to protect vital follow-on sealift, to allow swift STOW in littoral power projection operations, and to conduct any subsequent clearance or humanitarian operations. The ability to clear coastal waters, beaches, and inland areas of naval and land mines, specifically buried mines, is paramount to conducting any combat, peacekeeping, or humanitarian missions. [Ref. 6]

The following sections briefly describe current and emerging mine countermeasure methods available to amphibious forces or capable of being potentially fielded. The discussion is generally limited to the detection and destruction of buried mines or ordnance located in the shallow water, surf zone, and beach environments, also includes sea systems used in countering exposed mines. Land mines are usually emplaced in one of two methods, either buried or proud on the ground surface. Naval mines can be emplaced as buried, bottom, or moored mines. However, scouring action caused by the wind on land or the tides and current on the seafloor can quickly cover over exposed mines, adding to the difficulty of their detection. While several systems exist that can detect, counter, or sweep exposed mines, buried mines pose an extremely more difficult problem to naval and amphibious forces. Few technologies exist that can detect

buried objects, but their research, development, and fielding is of great relevance. Buried mines will be encountered in all spectra of warfare and the U.S. must possess effective countermeasure systems.

1. Current MCM Techniques and Technologies

Mine countermeasure techniques and technologies currently available to amphibious forces are somewhat limited in detecting buried mines. There is not one system that can detect buried mines within the very shallow water zone (~ 10 meters), beach areas, and inland approaches. While the easiest mine countermeasure technique would be to locate and avoid any mines, this method is not easily afforded to the force commander. He must be able to conduct rapid, in-stride breaching of detected mines and eventual clearance. Breaching operations involve detecting, locating, and marking or clearing mines in order to create a passage through the mine field. Clearance operations consist of detecting, locating, and neutralizing or destroying the mines to ensure safety in the entire mine field.

a) Water Mine Warfare Technologies

For mine countermeasure operations at sea and in the shallow and very shallow water zones, several systems are available:

- The *Avenger*-class (MCM-1) mine countermeasures ships capable of mine sweeping, mine hunting, and mine neutralization. This class carries a variable-depth mine hunting sonar and an unmanned mine hunting submersible vehicle capable of mine destruction or neutralization.
- The *Osprey*-class (MCH-51) coastal mine hunting ships, which also carry the variable-depth sonar and submersible vehicle.
- The MH-53E *Sea Dragon* airborne mine countermeasures helicopter which can tow a variety of mine sweep gear capable of detecting and sweeping mechanical, acoustic, and magnetic mines. [Ref. 7]

The above systems are only effective against floating, moored, or bottom-resting mines. They have no capability to detect buried mines or operate in the surf zone and beach area. However, they do provide the majority of mine clearance operations from the surf zone seaward. Should systems be developed that can detect buried mines in this area, they will probably be based upon these platforms. Other systems capable of operating in shallow water, the surf zone, and to the high-water mark that can be employed are:

- Diver systems (EOD, SEALs, or reconnaissance units) are capable of mine detection, destruction, and neutralization. Using hand-held probes and vision systems, they have limited detection capabilities and only very minimal ability to detect buried mines.
- Marine mammal systems (operating in shallow water and deeper operations) can detect and neutralize floating, moored, bottom, and buried mines.

It is interesting to note that the mammal systems are currently the only system capable of detecting buried mines. The U.S. currently possesses no system that is capable of detecting buried mines across the entire shallow water, surf zone, and beach environments.

b) Land Warfare Mine Countermeasures

Few systems are available for detection of buried mines from the beach area landward. Manual mine detection with hand probes or metal detectors still remains the most reliable method of mine detection. However, these methods are extremely dangerous, time-consuming, and not conducive to combat operations. Additionally, more and more mines are being manufactured almost entirely of non-magnetic materials, making detection extremely difficult with current metal detectors. Current methods for mine field breaching revolve around the "brute force" method:

- Mine clearing explosive line charges can create breach lanes approximately 14 by 100 meters. They are effective in the surf zone and inland.
- Track-width mine plows, fitted to M1A1 tanks, can also be used from the surf zone inland. However, the mines are only pushed to the side and remain active until neutralized.
- Shallow-water Assault Breaching System (SABRE) and Distributed Explosive Technology (DET) can be employed from Multi-Mission Craft, Air Cushioned (MCAC), for example, in the shallow water and surf zones. SABRE is an explosive line charge that can defeat mines in water depth up to 10 feet. DET is an explosive net system that can clear a square area (30 m by 30 m) in the surf zone and is used in conjunction with SABRE. Both can also be used on land. [Ref. 7]

While these systems cannot detect buried mines, they certainly can neutralize areas containing or suspected of containing buried mines. Other technologies available to detect buried mines include ground-penetrating radar (GPR) and explosive-sniffing dogs. However, GPR systems have to operate directly over the mines, which can be dangerous and their output is difficult for anyone but highly trained experts to interpret. Explosive sniffing dogs can be rendered ineffective by olfactory masking chemicals and their endurance is low. Both of these technological approaches suffer from low area search rates.

2. Emerging MCM Techniques and Technologies

Several systems and technologies are currently under development and may emerge in the future years as viable methods for the detection and localization of buried mines. Some of those systems are:

- Coastal Battlefield Reconnaissance and Analysis (COBRA) system with multispectral sensors to detect soil alterations for buried mine detection.

- Airborne Standoff Minefield Detection System (ASTIMID) which uses an infrared sensor to detect thermal contrast for visible mines and ground disturbances in the case of buried mines.
- Advance Mine Detection System (AMDS) utilizes HF sonar for bottom mine detection in shallow water. [Ref. 7]

Other methods are being investigated as to their applicability to detecting buried mines. Some of those methods are:

- The use of various spectra (infrared, visual, ultraviolet) to detect ground disturbances caused by mine emplacement.
- Microwave radiation to detect buried mines.
- Acoustic and seismic methods to detect buried mines.

The use of acoustic systems such as high frequency sonar to 'ping' at the sea floor and receive scattered signals back from a buried object is an ongoing research effort. However, this method is limited to short range in shallow water. Similarly, the use of seismic sources to produce vibrations that would scatter or reflect from a buried object is also being investigated. These reflected signals could be received, processed, and displayed, providing information as to the distance and bearing to the object. As previously stated, the object of this thesis is to do just that, to demonstrate the detection of buried mine-like objects from the reflections of seismic interface waves and to make target-strength measurements. The next section will detail some of the key issues faced in the conduct of this research and what may be one solution to the detection of buried mines.

C. OBJECTIVE OF RESEARCH

The concept of a seismo-acoustic sonar for the detection of buried mines and other ordnance was based on the research work conducted by ARL-UT [Ref. 2 & 3]. That research utilized the characteristics of seismic surface waves (Rayleigh waves) to

produce echoes from a mine-like object, which were recorded, processed, and analyzed. Analysis of these reflected waveforms yielded detection and target-strength measurements of the object. The successful results of that research yielded a strong conclusion that the seismo-acoustic sonar concept was feasible and that further research was warranted [Ref. 8]. Concurrent with research being done to fabricate, test, and implement a similar seismic wave generation source at NPS, this thesis will focus on detection and target-strength measurements of buried objects. The primary goal is the acquisition, processing, and analysis of seismic wave reflections in order to establish target-strength values and detection distances for a buried mine-like object. Some key issues that require attention and will be the focus of this thesis are:

- The development and refinement of signal processing methods in order to record, process, and analyze reflected target echoes or target-strength measurements.
- The establishment of target detection distances or minimum and maximum detection distances.
- Limitations of existing experimental equipment utilized in the research effort for this thesis, which will lead to improved research tools.
- The effects of the real-world environment, in which this research was conducted, on the experimental results.

From the work conducted by ARL:UT, several key problems arose that also must be addressed and overcome, if possible, in order for follow-on research to advance. A few of those problems are as follows:

1. Background Subtraction

The method of target detection, used by ARL:UT, entails recording a signal return of the ambient background without a target object present. Then the target is emplaced and subsequent signal returns are recorded. The two signal returns are then subtracted from each other, effectively canceling out any considerable background reverberation and

essentially leaving only the target return in the resulting signal record. This concept, while suitable for research work, is unfeasible from a military viewpoint. Another problem that exists with using background subtraction is it has no effect against noise. If noise is present in both the background and target records, then upon subtraction the noise is still present. If the noise is stronger than the target signal, the target will not be detected. A key objective of the present research is to demonstrate the detection of buried objects without doing background subtraction processing. [Ref. 8]

2. Low Target Return Strengths

The ARL:UT researchers observed that the echo returns from the buried object were exceedingly small. When compared against the ambient noise, the signal return from the target in an unprocessed data record was indistinguishable. Even with the use of background subtraction, the echo return was unremarkable. Several factors contributed to this problem: source signal strength, sediment attenuation of the signal and return, low receiver directivity, and physical characteristics of the target object. Each of these factors was taken into consideration and overcome for the present research work. [Ref. 8]

3. Vector Polarization Filtering

Seismic sources will invariably produce all types of waves (body and surface). To utilize only surface waves (Rayleigh) for propagation and reflection, the other unnecessary body wave modes (P & S), if present when received, must be filtered out. Vector polarization filtering permits the extraction of Rayleigh waves from the unwanted compressional and shear (P & S) waves because of the existing 90-degree phase shift between the vertical and radial components of motion. By using this phase relationship, vector polarization filtering computes a complex power with real and imaginary parts. Since the unwanted wave modes have components that are in-phase, they yield only a real component when the complex power is computed; the imaginary power part possesses information pertaining predominantly to the Rayleigh wave. This type of filtering becomes a necessary part to the problem of detecting buried objects using

interface waves. Using, understanding, and interpreting the results from this filtering process presents daunting challenge. [Ref. 8]

4. Summary

The purpose of the present research is to address and resolve some of the key issues mentioned above. With the successful detection of a buried mine-like object, tentative thresholds were established for target-strength measurements and detection distances. These thresholds, based upon the operational limits of utilized equipment, reflect the difficulties encountered in the successful completion of this project and the implementation of the system in a real-world beach environment. The results of this research prove that the concept of a seismo-acoustic sonar is valid and holds promise in its ability to detect buried mines.

The following four chapters will detail the steps taken to enable a successful demonstration of this concept. Chapter II details, briefly, previous research regarding the seismo-acoustic sonar concept. Chapter III describes the experimental equipment and procedures developed to support the acquisition of target detection data. Chapter IV focuses on the presentation of target detection data and the results of analysis. The final chapter provides conclusions and recommendations for future research efforts.

(This page intentionally blank)

II. PREVIOUS RESEARCH AND DEVELOPMENT

The following sections briefly detail recent and ongoing research efforts utilizing seismic waves. The majority of this work has entailed the use of surface waves in the beach sediment-air interface to detect and localize buried objects. These experimental projects have formed the basis from which this thesis work has moved forward. Much work has been done in the development of various excitation sources for seismic interface waves and in the use of these sources for detection, producing target-strength measurements, bearing, and distance to various objects.

Before reviewing the seismic sonar literature, it should be mentioned that there has long been a concerted research and development effort at the Naval Coastal Systems Station in Panama City, Florida, to develop a synthetic aperture sonar that can be "sensor fused" with magnetic sensors for the detection of mines buried seaward from the surf zone. Two excellent articles on these sensor approaches, one by G.S. Sammelman, et. al. (synthetic aperture sonar) and another by T.R. Clem (magnetics), recently appeared in an Office of Naval Research publication Naval Research reviews, D. Toderoff Ed., vol. XLIX, b. (3), 1997. [Ref. 9]

A. RESEARCH AT NPS

1. Buried Object Detection

The first research project to be conducted at NPS utilizing surface waves was done by a student, Lt. William Stewart, in 1995. The goal of that research was to evaluate the use of surface waves to detect buried objects. This research included the development of a surface wave source and receiver, the use of multiple sources forming an array to enable beamforming, and target localization using a single source and a multiple element receiver. The source utilized in this work was a 4-in (10-cm) diameter electrodynamic woofer speaker with a frequency response of 50-7,000 Hz. Additionally, the speaker had an aluminum, cone-tipped appendage attached to the center of the

speaker diaphragm, along with a 0.055 lb (0.025 kg) mass. The purpose of the cone and mass fixture device was to improve the transfer of the vibratory motion of the speaker diaphragm to the ground. The source device is depicted in Figure 2.1. [Ref. 10]

The receiver array consisted of three single-axis geophones, or seismometers, to detect ground vibration. Experiments were conducted in a 5-ft (1.5-m) tall wooden water tank with a diameter of approximately 13 ft (4 m). The tank was filled with typical beach sediment-type sand procured locally from the shoreline. The target for this experiment was a copper cylinder of height 1.2 in (3 cm) and diameter 4 in (10 cm). It was placed vertically in the tank with approximately 0.8 in (2 cm) of sand covering the top end. Background subtraction was applied to the received signals, to locate the buried object. A number of signal pulses from the source were received without the target present.

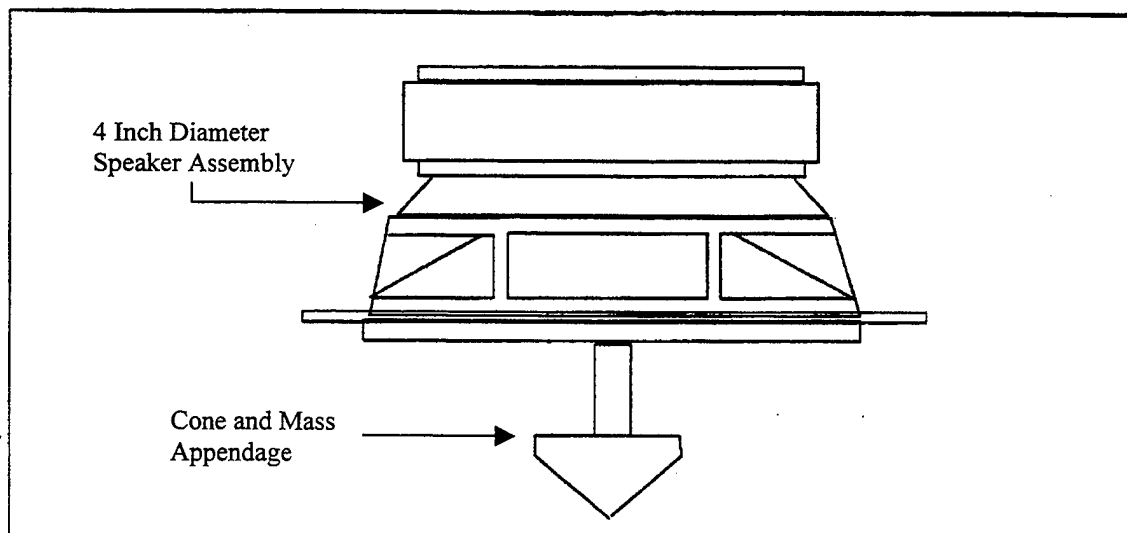


Figure 2.1. Seismic source design, after Ref. 10.

These records were then summed and averaged to produce a single averaged background record. A similar procedure was followed after the target was emplaced. The resulting background record was then subtracted from the target record to produce a localization of the target. By calculating the speed of the Rayleigh wave from the length of the source-

receiver direct path, the length of the reflected path (source-target-receiver) can also be determined. Together these two paths form an ellipse of possible locations of the target. Using an array of receivers, multiple ellipses can be produced, with the intersection of these ellipses providing target location. By using a single seismic source, a three-element receiving array, and the background subtraction signal processing technique detailed above, Lt. Stewart was able to demonstrate target localization. [Ref. 10]

2. Discrete-Mode Source Development

Work done recently at NPS by Lt. F.E. Gaghan, in March of 1998, concentrated on the development of a seismic source that preferentially excites interface waves. The design, fabrication, and field testing of several source systems to selectively excite the desired waves was the goal of his work. Because seismic interface waves have an elliptical particle velocity, which orbits in the vertical plane containing the direction of propagation, a source inducing elliptical motion at the interface can be expected to selectively produce the desired Rayleigh waves. Two types of seismic sources were developed in this work. The first was a small electromagnetic shaker assembly, coupled to the ground by a hollowed-out aluminum block. This assembly was utilized as a proof-of-concept demonstrator for work in the laboratory. The two shakers were mounted at 45-degree angles to the normal on top of the block. The block was partially buried in the sand to achieve coupling. The sand tank utilized in Lt. Stewart's work was also used here. The shakers provided an output of 0.2 lbf (0.89 N) with a frequency range of 100-1000 Hz. In this experiment Lt. Gaghan was able to selectively excite exclusively only vertical or horizontal motion with this source. The source device is shown in Figure 2.2. With these promising results, Lt. Gaghan proceeded to develop a larger prototype shaker source. [Ref. 4]

The second source developed consisted of a series of modifications to a basic design incorporating two electromagnetic vibration transducers. These vibration devices are referred to as Bass shakers and are used for low frequency vibrations in car stereo systems. The shakers have a nominal output force of 10 lbf (44.5 N) and frequency range of 20-100 Hz. The shakers were mounted on an aluminum plate at 45-degree angles to

the normal. The plate served both as a mount for the shakers and as a coupling device to the sediment. It was designed with several 6-in (15-cm) machine screws at various orientations, which were screwed into the sediment each time the device was emplaced. The source device is shown in Figure 2.3. [Ref. 4]

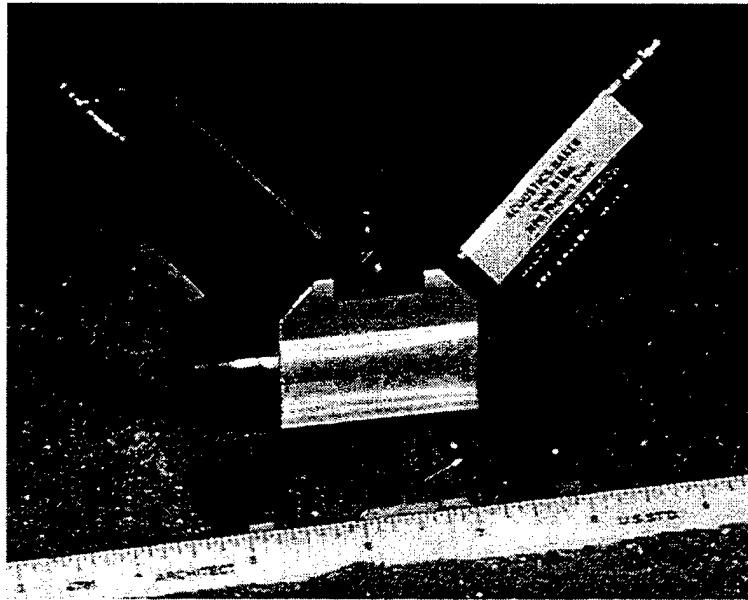


Figure 2.2. Lab source design, from Ref. 4.

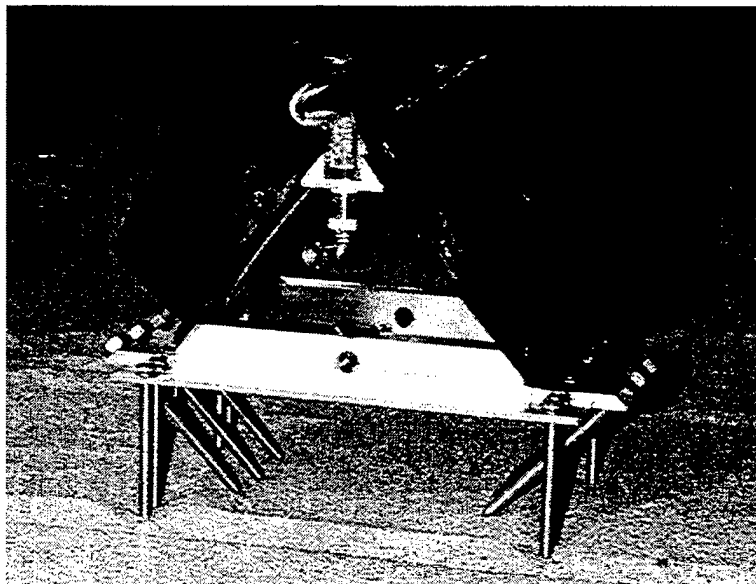


Figure 2.3. Field source design, from Ref. 4.

By controlling the phase, amplitude, and frequency of each shaker, two-dimensional oscillatory motion could be excited. This mimicked the elliptical particle velocity of Rayleigh waves and served to discretely excite this motion at the interface of beach and air. The source was driven under several different modes of excitation, but it was observed that multiple types of interface and body waves were generated. Regardless of various input excitation parameters, all types of seismic waves were present. However, there was no automatic feedback control employed to suppress the unwanted modes, a suggestion forwarded by Lt. Gaghan for follow-on work. One interesting observation showed that the beach medium itself acted as a filter, quickly attenuating any body waves while the interface waves continued to propagate a substantial distance. [Ref. 4]

This research exhibited the difficulty of discrete-mode excitation of Rayleigh waves. Some conclusions drawn by Lt. Gaghan include the need for higher quality, greater force-producing excitation sources and a better sediment-coupling device. Another recommendation was that sources intended to excite out-of-phase horizontal and vertical motion should be oriented in those directions. [Ref. 4]

B. RESEARCH AT ARL-UT

As mentioned previously, the work done by ARL-UT demonstrated the concept of a seismic sonar for the detection of buried mines and other ordnance. The seismic wave source used by ARL-UT consisted of an electro-mechanical transducer and ground-coupling device. The transducer was made up of an oscillator, linkage assembly, and coupling device, which provided seismic vibrations to the ground and stabilized the source. The coupling device consisted of an array of 1.6 in (4 cm) carpentry nails attached to a coupler plate, or "foot", that rested on the beach. The receiver array consisted of a three-element array of triaxial seismometers. The entire experimental setup is shown in Figure 2.4. [Ref. 8]

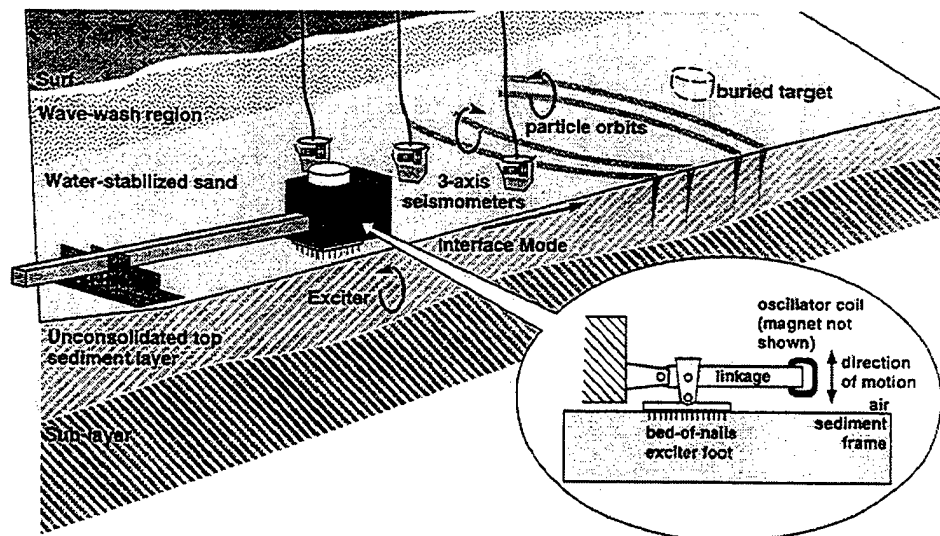


Figure 2.4. ARL-UT seismic sonar experiment, from Ref. 8.

The mine-like object used as a target in this research was a titanium cylinder 8 in (20 cm) in height, 8.7 in (22 cm) in diameter, and mass 77 lb (35 kg). When buried in the beach sediment for detection, the cylinder was oriented vertically, with its top end flush with the sand surface. During the course of signal processing, ARL-UT found that the signals observed at the receivers contained significant reverberation that masked the target echo. To overcome this, they used coherent subtraction (subtracting the signal representation of the background from the signal with the target present) to isolate the target echo or scattering. Another concept utilized by ARL-UT was vector polarization filtering. The vertical and radial components of a Rayleigh wave are naturally 90 degrees out of phase, while for the other types waves, unwanted for target detection, they are in phase. By filtering for this phase difference, essentially only the preferred interface Rayleigh wave signal remains. Using these techniques, ARL-UT was able to successfully detect and localize the mine-like object target. [Ref. 2]

Concurrently developed with the fieldwork by done by ARL-UT was a theoretical examination of the scattering of interface waves from pointlike obstacles. The model created through a perturbative computation predicts that scattering from a target in an unconsolidated sediment medium, such as beach sand, should be dominated by the target

mass. Target-strength levels are predicted using the model and reasonably agree with those found in the experimental results. [Ref. 3]

C. UNDERWATER EXPERIMENTS USING SONAR

Several experiments have investigated the scattering of sound by objects buried in underwater sediments. By using acoustic sources and receiver arrays located in the water, the detection of buried objects has been demonstrated, but only at high grazing angles, incompatible with military applications. Elastic objects buried in ocean sediments display a scatter behavior similar to those located in water. However, this scattering is affected by interface proximity and sediment attenuation and loading. Because of this related behavior, it is theorized that classification as well as detection of buried objects in the seafloor is possible. [Ref. 11 & 12]

Similar research has also been conducted using broadband, dolphin-like sonar signals to classify buried targets. Capitalizing on the dolphin's ability to use its sonar to detect buried prey, a sonar transducer emulated these signals to detect and classify buried objects. Various elastic objects, ranging from cast iron to glass, were detected and identified with approximately a 75% success rate. However, this method is not suitable for military applications. [Ref. 13]

D. CURRENT RESEARCH AT NPS

Currently at NPS, Lt. S.M. Fitzpatrick [Ref. 14] is conducting related research work. His research involves the development, fabrication, and testing of a seismo-acoustic sonar source that would be used in the detection of buried objects. The seismic source developed by Lt. Fitzpatrick provided the generated interface waves utilized in this thesis for detection and target-strength measurements of buried objects. Details of the development of this source and how it was integrated with other equipment to achieve the collection of data is presented in Chapter III. Also provided is information concerning general experimental procedures, signal processing methods, and a description of how target detection experiments were conducted.

(This page intentionally blank)

III. RESEARCH METHODOLOGY

Concurrent with the research work presented in this thesis was the actual fabrication, development, and testing of a new seismic wave generation source. Lt. S.M. Fitzpatrick did this work at NPS as his thesis research for joint Master of Science degrees in Applied Physics and Mechanical Engineering. This work was follow-on research and development along the lines of Lt. Gaghan's thesis work that was previously mentioned in Chapter II. Solving the problems associated with the development of a discrete-mode excitation source for surface waves, specifically Rayleigh waves, and the requirement for greater force-producing sources provided the basis for Lt. Fitzpatrick's thesis. Much of the development and field testing work of the seismic source was done jointly by Lt. Fitzpatrick and myself. With the success of target-strength measurements so dependent upon the source, much time was spent on source development and testing.

The following sections briefly describe the development of the seismo-acoustic sonar source and other equipment used to generate, receive, process, and analyze the seismic wave signals in order to detect a buried object. Also discussed will be a general overview of experimental procedures pertaining to the numerous field experiments conducted over a six-month period. This will be followed by a detailed discussion of the digital signal processing methods utilized to collect, process, and analyze the raw field data. Also presented will be information regarding equipment set-up and configurations developed for the target detection experiments. Finally, a sample of the raw data will be presented as a bridge to the next chapter that will detail the successful target detections, yielding target strength and localization information.

A. SOURCE DEVELOPMENT

The seismic sources developed and modified for this thesis research were two 25-lbf (111 N) electro-mechanical linear actuators built by Aura Systems, Inc., of El Segundo, California. The specifications and operating parameters for the basic, unmodified actuator are provided in Appendix 1. The actuator in its basic configuration is shown in Figure 3.1. Several modifications were performed to each actuator to include

the addition of fixed weights, movement of electrical connections, and application of ground coupling devices. For field experimental work, each actuator was placed in a fabricated PVC pipe container, sealed, and waterproofed. This final configuration, which was used in the execution of all field experiments, is shown in Figure 3.2. Much greater detail relating to the design and testing of these seismic sources is contained in Lt. Fitzpatrick's thesis [Ref. 14].

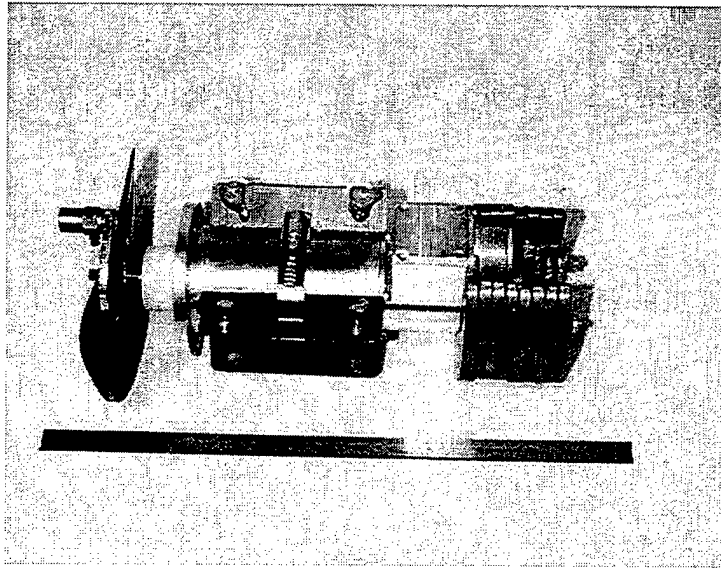


Figure 3.1. Aura 25-lbf Electro-mechanical linear actuator.

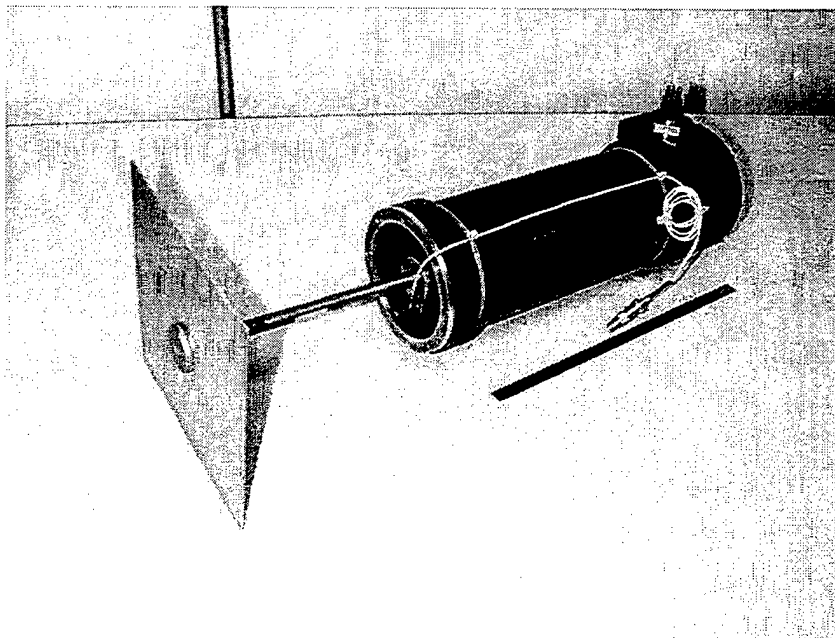


Figure 3.2. Actuator with waterproof case and coupling device.

B. DATA COLLECTION EQUIPMENT

An Aura Systems Electronic Control Unit (ECU) controlled each of the two actuators described above. A Hewlett-Packard (HP) 3314A Function Generator provides a waveform of desired amplitude and frequency to each control unit. A master-slave relationship allows one function generator to provide signal triggering for the other and for the entire signal generation and receiving system. The generated waveforms are initially band-pass filtered with Krone-Hite (H-T) 3202R filters and amplified with Stanford Research (SR) SR50 pre-amplifiers prior to being passed to the respective actuator control unit. For some experimental set-ups this filtering and amplification step was bypassed and the generated waveform was applied directly from the function generators to the control units. An explanation for this procedure will be addressed in the signal processing section. The above electronic components constitute the entire signal generation suite of equipment.

The seismic signals are received by two tri-axial moving coil seismometers. The received signals are pre-amplified with a gain of 40 dB. A uni-axial accelerometer (PCB model 353B03) is attached to each sediment-coupling plate on the actuators. This accelerometer is used to provide a representative output of the movement of the coupling plate as it responds to the waveform input to the actuator. The two accelerometer signals are also amplified with a PCB 482A17 amplifier, filtered with K-H filters, and together with the six seismometer outputs, eight channels of data information are available for recording and analysis. This data are recorded using a SPS model 390 8-channel Signal Analyzer. The 390 is a Pentium® computer using a 120-MHz processor, Windows® 95, and operating a signal analysis software package. All eight channels of data can be viewed simultaneously and can be manually or continuously updated based upon a triggering signal from the function generator. A Philips PM3384 oscilloscope is used to view various signal waveforms generated or received at numerous stages in the data flow. Also used for near-real time signal processing and analysis was a Dell Pentium® laptop computer using a 233-MHz processor, Windows® 98, and MATLAB® 5.0. The above electronic instruments constitute the signal-receiving suite of equipment.

Each equipment suite is mounted in a separate equipment rack to isolate signal generation electronics from signal receiving electronics. This configuration also greatly

contributed to ease of handling and transportability. Transportation to and from the field research site was provided by a 30-foot recreational vehicle (RV) owned by the NPS Oceanography Department and under temporary loan for the duration of this thesis work. The vehicle met all requirements, providing the necessary space and electrical power, with an on-board generator, for experimental research. An additional vehicle was procured during the field experiments to increase the mobility of the research equipment. A John Deere 6x4-wheel drive TrailGator[®] utility vehicle was purchased to improve research site access. The TrailGator[®] provided the flexibility to locate all the research equipment and electronics right at the test site. The vehicle provided a bed to transport all equipment and to mount both equipment racks during data collection. As detailed later, this enabled signal processing and analysis in near-real time right on the beach. This negated the need to constantly traverse the bluff to adjust equipment. The RV provided only electrical power. A typical configuration with equipment racks mounted and operating, representative of normal experiment set-up, is shown in Figure 3.3. The next section discusses some of the preliminary and general procedures utilized prior to the conduct of experiments.

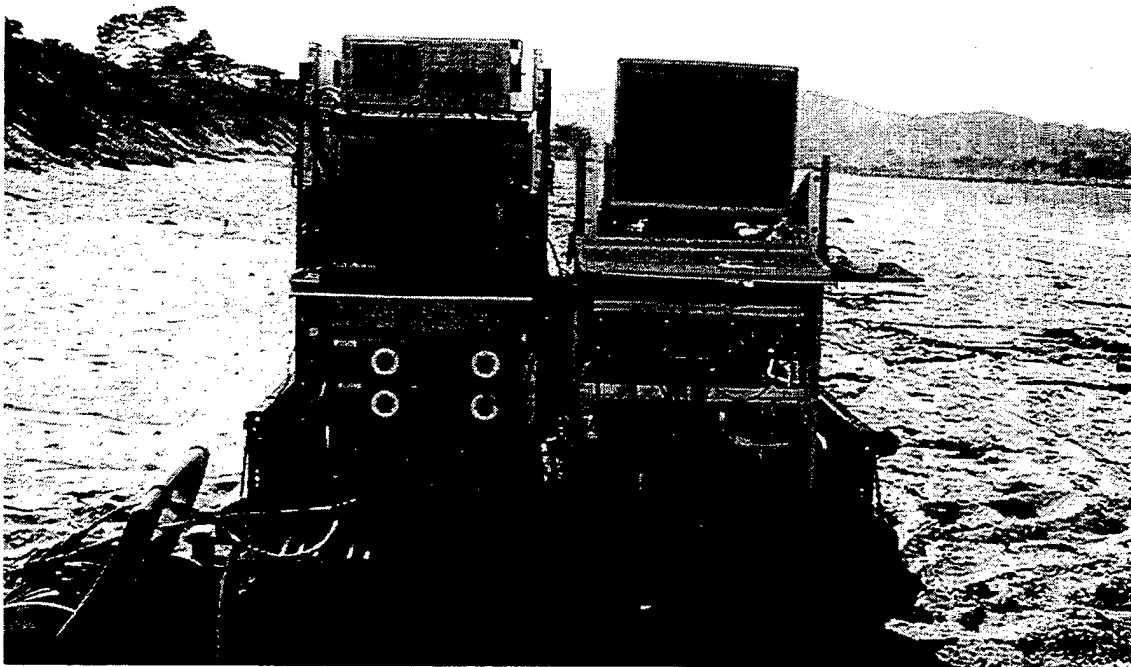


Figure 3.3. Equipment configuration for data collection.

C. GENERAL EXPERIMENT INFORMATION

The following sections will address some common aspects of the majority of the field research experiments. Approximately fifteen separate days were spent on the beach conducting experiments to detect a buried object. Each of these days is considered a separate experimental event. While certain characteristics and events of a particular experiment made it unique, other procedures and processes were common throughout the research. Discussed below is the beach research site used throughout this thesis work, and its characteristics. Also discussed are the mine-like objects that were used for target detection and some current mine information. Additionally, some of the preliminary procedures conducted for each experiment are discussed.

1. Research Site Characterization

The beach site used over the course of the entire field research phase was a stretch of U.S. Navy-owned beach directly seaward of NPS. This area, commonly referred to as the 'Navy Beach', is similar to the majority of coastal beach areas of the Monterey Bay, and is open to the public during daylight hours. Throughout the course of all experiments, the same stretch of beach was consistently utilized. This area measured roughly 150 feet in length running parallel to the waterline and varied from 20 to 50 feet from the high- to low-water mark, depending on the tidal cycle. A 30-foot shear bluff backs the relatively flat sandy area of the beach. This area with normal equipment configuration is shown in Figure 3.4.



Figure 3.4. Beach test site with data collection equipment.

The beach is consists of a fine, unconsolidated sand, with a uniform consistency throughout. The density and moisture content varied with distance from the waterline and with tidal cycle. From one experiment to the next, sand characteristics of the test site were rarely similar. During any particular data collection event the test site may consist of a few inches of dry, loose sand overlying wet, hard-packed sand. Conversely, during a separate test event, the site may consist of completely wet, hard-packed sand, recently washed-over by the tide. This variability and its impact on collected data will be discussed later.

2. Targets

The goal of this thesis is the measurement of the target strength of buried mine-like objects due to the scattering of seismic interface waves. As mentioned in the Introduction, there are countless types of both land and naval mines. They vary in size, mass, and material from plastic anti-personnel mines of a few ounces to cast-iron naval mines weighing thousands of pounds. The U.S. possesses relatively few types of land and naval mines. The land mines consist of the M16 anti-personnel mine, the M15 steel, M19 plastic, and M21 tilt-rod anti-tank mines. An inert example of each mine is shown in Figures 3.5 (M16 and M21) and 3.6 (M15 and M19).

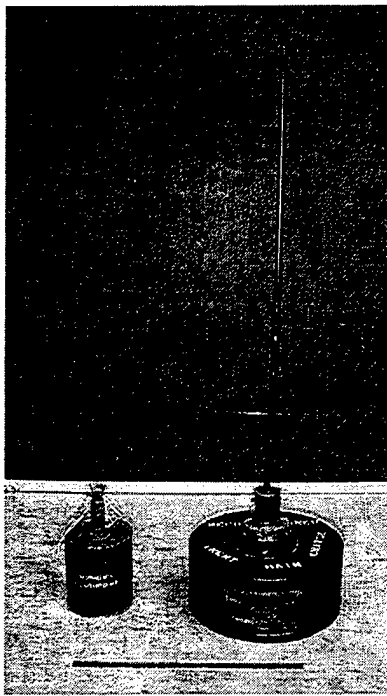


Figure 3.5. M16 and M21
U.S. land mines.

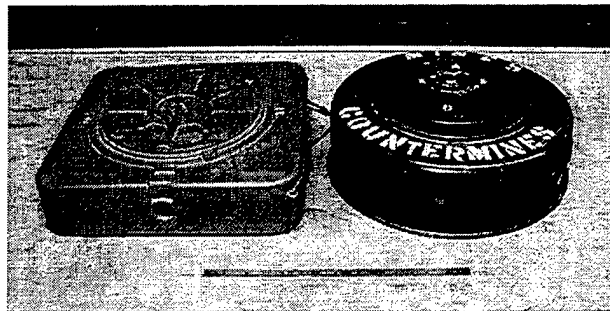


Figure 3.6. M15 and M19 U.S. land mines.

Throughout the world military forces there are countless types of land mines in production, in inventories, and being exported, both anti-personnel and anti-tank. While U.S. forces will not probably encounter their own mines in warfare, their presentation here typifies other countries' mines in use around the world and provides a basis for the present research in mine detection.

The principle types of naval mines in the U.S. inventory consist of either moored or bottom mines. The Mk 60 CAPTOR mine is a moored mine capable of launching an acoustic-homing torpedo against submarines. The Quickstrike-series of aircraft-laid bottom mines are conversions of the Mk 80-series bombs. The Mk 62 is a modified Mk 82 500-lb (227 kg) bomb and the Mk 63 is a modified Mk 83 1000-lb (454 kg) bomb. However, the Mk 65 Quickstrike, weighing 2000 lb (908 kg), was specifically designed as a bottom mine. The Mk 67 Submarine-Launched Mobile Mine (SLMM) is a self-propelled bottom mine that is based on a modified Mk 37 torpedo. [Ref. 15]

There are a few foreign naval mines that may figure prominently in mine countermeasure operations and are worth mentioning. The first is an Italian mine, the Manta, which is a bottom influence mine. This mine has been exported to such countries as Iraq and the Peoples Republic of China. It is believed that it was a Manta mine that damaged the USS Princeton during the Gulf War. Another mine of interest is the Swedish anti-invasion mine, the Rockan, which also is a bottom influence mine. Used in shallow water against amphibious landing and other craft, it also has been exported.

The work done by ARL-UT [Ref. 2 & 3] suggests that target strength levels and wave scattering from a buried object are dependent on the size and mass of that target relative to the surrounding medium. It is obviously unfeasible to use live mine ordnance as a detection target, and so surrogate, mine-like objects had to be found. To make its detection as easy as possible, a target must be as large and massive as possible, yet not a burden to move and emplace. Two such objects were utilized in this research effort.

The first mine-like object was a discarded gas cylinder weighing 150 lb (68 kg). The cylinder was approximately 5 ft (1.5 m) long, 8 in (20 cm) in diameter, with a 1/4-in (0.6 cm) wall thickness. The second object was a U.S. Navy power can or "powder keg" in the shape of a cylindrical sheet metal can 18 in (46 cm) high and 24 in (61 cm) in diameter, weighing 16 lb (7 kg). The gas cylinder was modified by cutting off one end and installing a watertight collar and mating device for reattachment. This was done to enable additional weight to be placed inside the cylinder and still maintain watertight integrity if buried in the surf zone. Similarly, the powder keg had a removable top with watertight seal that facilitated weight addition. The powder keg and cylinder are shown in Figures 3.7 and 3.8 respectively. The additional weights used consisted of a number of



Figure 3.7. Powder keg target with lid open to show access.

lead blocks, each weighing 26 lb (12 kg). The gas cylinder and powder keg could hold 18 and 24 blocks, respectively. This made the maximum weight of the cylinder and blocks 618 lb (280 kg) and the powder keg and blocks 640 lb (290 kg). While similar in mass, each object provided a different aspect to the oncoming seismic waves. The cylinder was always buried on its side with the cylindrical axis horizontal and normal to the direction of wave propagation. The powder keg was always buried upright, with the cylindrical axis vertical and normal to the wave propagation direction.

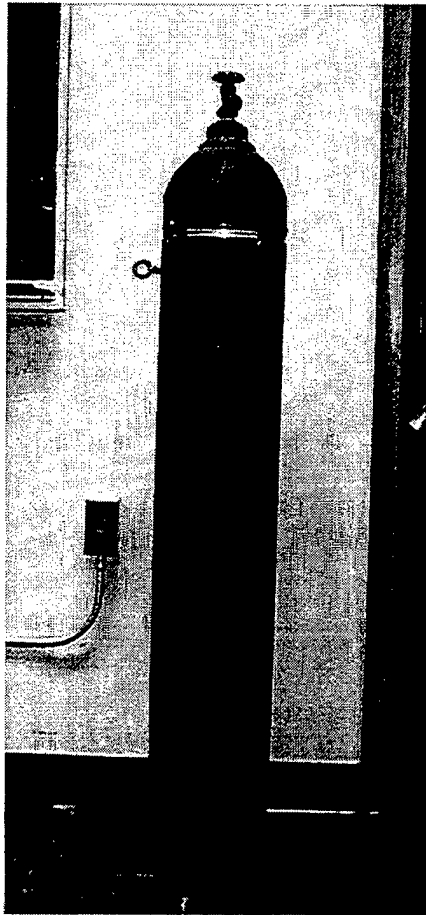


Figure 3.8. Gas cylinder target.

3. Preliminary Procedures

The procedures for conducting data collection experiments were similar throughout the course of this research work. The recreational vehicle, containing all electronic instruments, would be positioned at the bluff edge overlooking the beach site. The seismic source actuators would be emplaced on the beach in a level and debris-free site and cabling connected them to the ECU's. Both actuators are oriented vertically with the coupling plates buried a minimum of 6 in (15 cm) in the beach sediment. Cabling connecting the uni-axial accelerometers (attached to the coupling devices) would also be connected. In similar fashion, the seismometers would be emplaced on the beach. All respective sets of cabling used were approximately 150 ft (45 m) in length to provide

flexibility in reaching separate areas of the test site. At this point two important characteristics of the test site were determined, the best frequency for surface wave propagation, and the surface wave speed.

a) *Determination of Optimum Propagation Frequency*

As previously discussed, beach conditions (sand density and moisture content) varied in time. An overarching goal for every experiment was to put as much energy into the sediment as possible. This is accomplished by finding the best frequency possible for maximum wave propagation, given the beach conditions during a particular experiment. Finding and using the optimum propagation frequency enhances the chances of target detection. Creating conditions whereby the strongest possible incident surface wave is reflected by the buried target, the probability of detection of those reflections only improves. In initial experiments, a source signal frequency of 100 Hz was used, but it was observed that the received signal voltage levels at the seismometers were not consistent from one day to another. This inconsistency led to efforts to find the optimum wave propagation frequency for each day experiments were conducted.

Finding the optimum propagation frequency proved to be a relatively simple task. The process involved incrementing the source signal frequency in 5-Hz steps, usually between 50 and 120 Hz. The resulting received signal amplitude varied considerably with frequency. By observing the received signal, continuously updated on the 390 Signal Analyzer, the maximum amplitude and corresponding frequency could be determined. In effect, the beach sediment determined the best signal frequency to use on that specific day. This process was performed each experiment day, providing a specific 'best' frequency. The optimum frequency usually fell between 70 and 90 Hz.

b) *Determination of Surface Wave Speed*

The wave speed of the surface seismic waves also varies. On each experimental day, a wave speed measurement and calculation would be performed. Here a number of received signal sets would be recorded, with the seismometers placed at incremental distances from the source (~10-80 ft) (~3-24 m). The records would be

converted to MATLAB files, then averaged, summed, and filtered to eliminate noise. The resulting files, each pertaining to a particular distance from the source would be time correlated against each other using a MATLAB program to determine an average wave speed for that particular day. The determination of optimum frequency and corresponding wave speed figure prominently in the signal processing techniques to determine target strengths of the buried objects.

D. SIGNAL PROCESSING METHODS AND TARGET DETECTION EXPERIMENTS

The following will be a discussion of the general execution of a field experiment. Approximately 10 days of experiments were spent on the beach collecting target detection data prior to the first confirmed detection. Numerous equipment configurations, signal processing methods and seismic wave generation, propagation, and receiving techniques were tried in an attempt to detect the buried objects. After several months of experimental trial and error, target detection was achieved, and numerous follow-on detections were made. The next section discusses the signal processing methods utilized throughout each experiment and how the raw data are processed to provide target-strength measurements. The following section explains the general procedures conducted during target detection experiments.

1. Signal Processing Methods

Past efforts to detect buried objects utilized background subtraction to see the signal backscatter from the target. A fundamental goal of this thesis work is to detect the target without using that method, which is impractical for military applications. By developing a better seismic source, one that induces stronger surface waves in the sediment, a greater amount of energy arrives at the target, increasing reflection strength. By refining experiment and signal processing procedures, the reflection should become more apparent and easier to identify, providing far more accurate target strength and localization information. The actuator sources developed by Lt. Fitzpatrick, which can provide up to 25 lbf (111 N), were limited in their output by the voltage supplied (10 v)

by the function generators. This resulted in an output of approximately 15 lbf (67 N). Attempts to amplify this voltage output to utilize the full capacity of the actuator were unsuccessful. The pre-amplifiers utilized were constantly overloaded and the resulting waveform was distorted.

a) Source Signal Generation and Processing

Initially, the source signal waveform, generated by the HP Function Generator, was filtered and pre-amplified prior the actuators. The signal was band-pass filtered at 50-200 Hz to remove low and high frequency components and produced a clean waveform. Because of voltage limitations on the K-H filters and SR pre-amplifiers, the maximum signal amplitude was approximately 12 volts. Above that level there was significant waveform distortion and overloading of the pre-amplifiers. During the course of data analysis, it was discovered that signals sent directly to the actuators from the function generator, with a peak amplitude of 10 volts, received and band-pass filtered using MATLAB were of similar quality and amplitude as the previous signals. Subsequently, this latter method was used in follow-on experiments.

b) Received Signal Processing

The signals received during each experiment were three channels (x-, y-, and z-axis) of data from each of the two seismometers and the two channels (z-axis) of data from the uni-axial accelerometers mounted on the sources. Each received signal from the seismometers was recorded as received, and later filtered using MATLAB routines during analysis. The signals received by the accelerometers were amplified and band-pass filtered at 50-200 Hz using the K-H filters. The eight channels of data were collected and recorded by the SPS 390 Signal Analyzer. Each channel was also displayed on an associated computer monitor and updated as required. The signals were recorded as a .XRC file. The .XRC, or Extended Record, file was transferred to the laptop computer using a transfer cable, and converted to a MATLAB data file using a utility program supplied by SPS. All subsequent signal processing and analysis was done digitally using MATLAB. In most instances, during all experiments, signals were

recorded in sets of ten. This resulting set of records was later time-averaged, producing one record representative of the set. Filtering could also be applied during this process. An example of averaged, unfiltered data received is shown in Figure 3.9. This shows all eight channels of data. The data are a time-averaged set of 10 records of the scattering from the powder keg target loaded with 24 lead blocks. The receiver was at 10 ft (3 m) from the source and the passing source signal can be seen at that distance. The target was at 22 ft (6.7 m) (round trip distance) and is indistinguishable in these records.

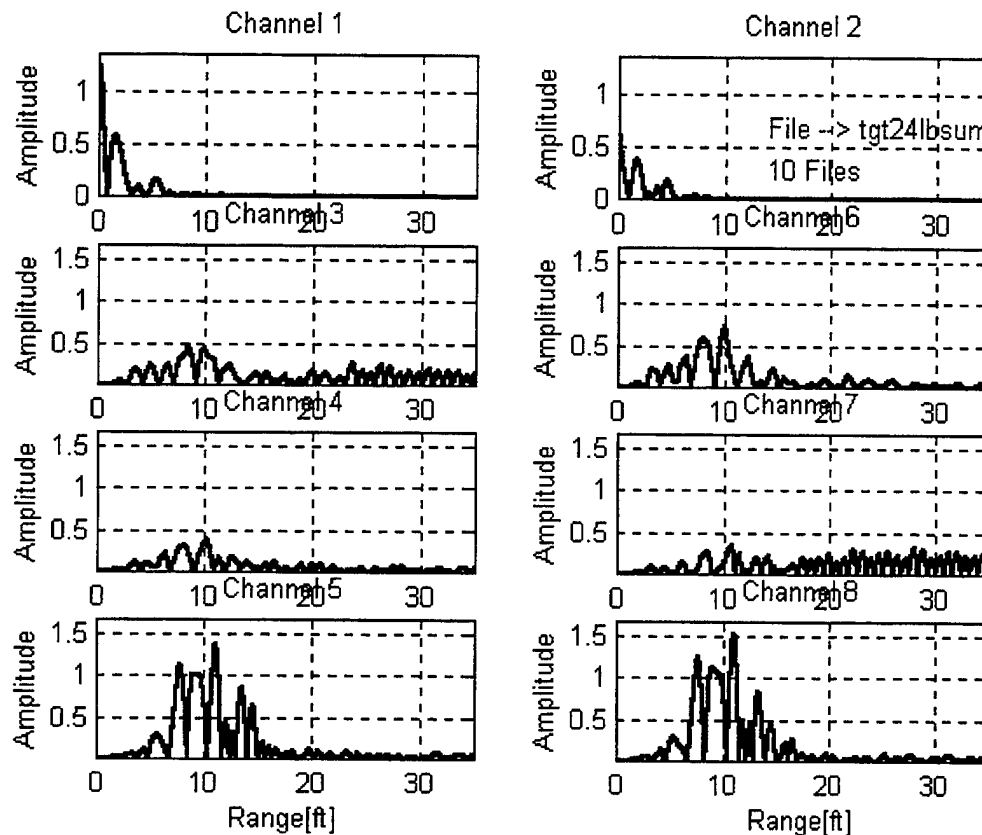


Figure 3.9. 8-Channel data plot of received signals.

c) *Signal Analysis*

Each data record is recorded, converted, processed, and filtered. The resulting file can then be analyzed for target detection. MATLAB programs were utilized for all the signal analysis work. The most simple analysis tool for detection was to visually inspect a plot of all eight channels of data. In several experiments, a set of

received signals was recorded with no target present. A similar set of signals was recorded with the target present. The records were then visually compared. Since the distance to the target is known, the resulting amplitude of the reflected signal should be visible at the proper distance or time if the reflection signal is strong enough to stand out from the noise. Normally it was not possible to distinguish the target reflection clearly in the data record in this manner. Even by using background subtraction, the reflection was not apparent. Because of this continual problem, the use of vector polarization filtering became a prerequisite for successful target detection.

Vector polarization filtering, as previously mentioned, permits the extraction of Rayleigh waves from the unwanted compressional and shear (P & S) waves, because of the existing 90-degree phase shift between the vertical and radial components. This filtering is done digitally using MATLAB and the Hilbert function. The MATLAB Hilbert function transforms the real measured data into a phasor. The Hilbert is applied to the radial and vertical components of the signal, and the (complex) "crossed-power" function can be computed, given as;

$$\underline{P}_{rv} \equiv \underline{r}_{\text{hilbert}}^* \times \underline{v}_{\text{hilbert}} \quad (3.1)$$

Because of the 90-degree phase difference between the radial and vertical components of motion in a seismic interface wave, the imaginary component of \underline{P}_{rv} is essentially proportional to the intensity of the seismic interface wave. The polarity of the imaginary crossed power yields the polarity of the elliptical particle motion associated with the seismic interface wave; a positive value of the imaginary crossed power corresponds to prograde elliptical particle motion, a negative value corresponds to retrograde motion.

As mentioned previously, the rotation of an interface wave can be prograde or retrograde depending on the wave depth. An example plot of the imaginary crossed power is provided in Figure 3.10. Looking at the imaginary power plot, the passing of the incident wave past the receiver at 10 ft (3 m) is clearly visible. The reflection of the target, located at 22 ft (3 m) (round trip distance, defined below), is not visible at this scale.

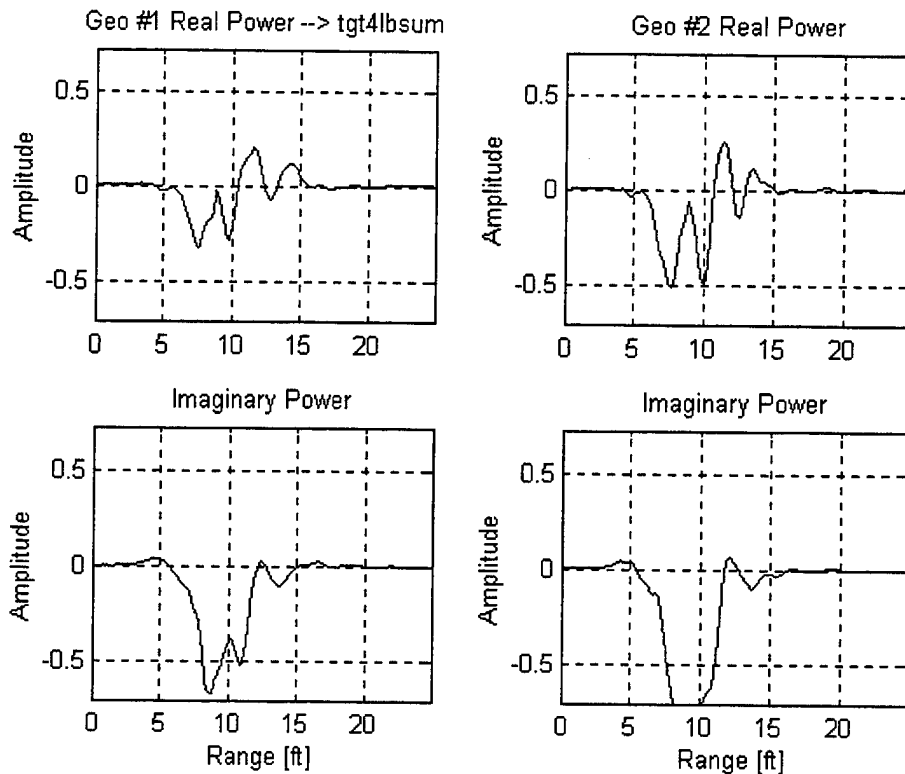


Figure 3.10. Crossed power plot of received signal.

2. Target Detection Experiments

Once the procedures for successful detection were established, similar procedures were instituted for each subsequent experiment. After equipment set-up, preliminary procedures are conducted to determine the optimum propagation frequency and corresponding surface wave speed characteristic to the test site on that particular day. As mentioned, these parameters changed from day-to-day. After these events, a set of received signals, with no target present, was evaluated using vector polarization filtering. This was done to establish the quiescent point of the received signal as it passed the seismometer receiver. Referring to Figure 3.10, this quiescent point would be defined as a point where little deflection of the imaginary power remained, caused by the passing of the incident wave at the receiver. Determination of this point, estimated by visual inspection of the crossed power plot, provided a round-trip distance at which to bury the

target. Typically, the target was emplaced at a distance of 11 to 16 ft (3.3 to 4.8 m) from the actuator sources. This round-trip distance is the entire distance traveled by the wave as it propagates from the source to the target, scatters, and is received at the seismometer receiver. The receivers were typically placed six feet from the sources, providing source-target-receiver distances of 20 to 26 ft (6.1 to 7.8 m). The particular configuration during any given day did vary from the distances given above, but only by a few feet. A schematic of a typical configuration is given in Figure 3.11.

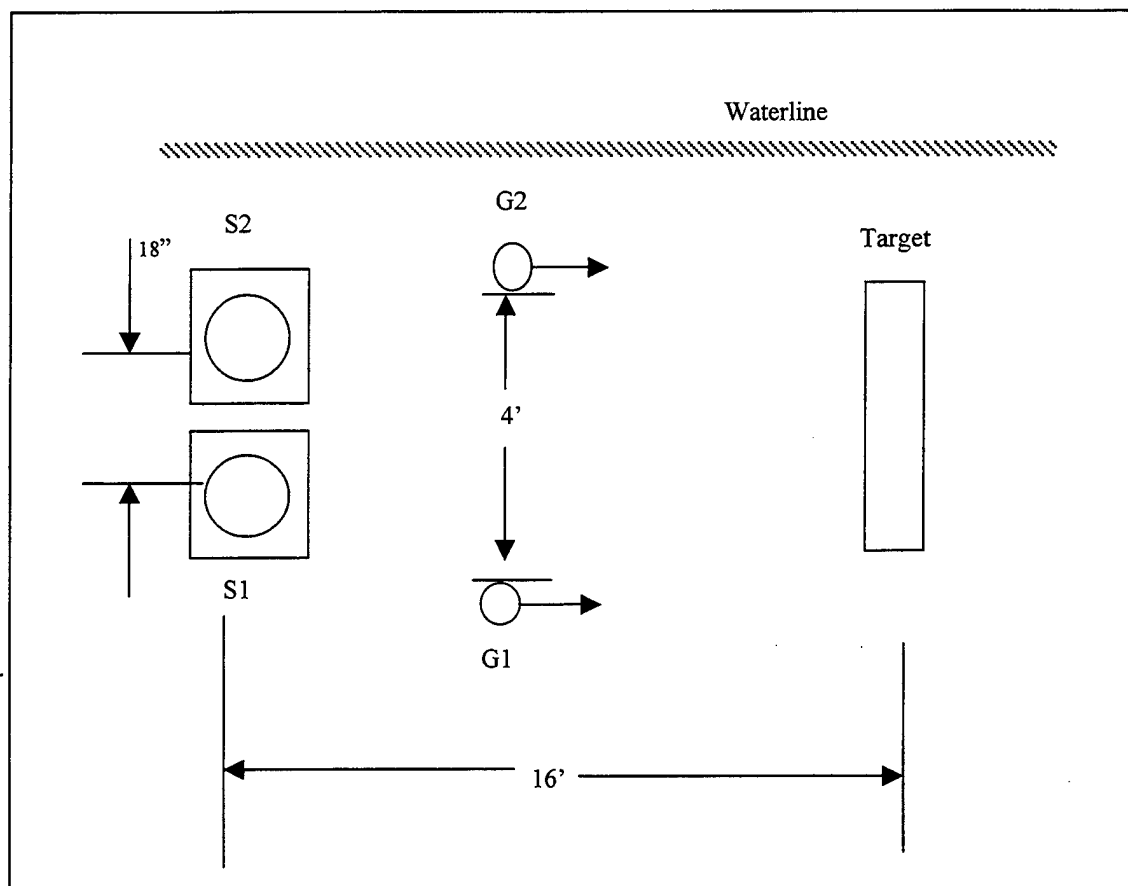


Figure 3.11. Typical equipment configuration for target detection, not to scale.

The four processes detailed above, determination of optimum propagation frequency, determination of corresponding surface wavespeed, determination of target distance, and equipment configuration, now allowed the target to be emplaced. The target (power keg or cylinder) was buried at the proper range by digging a hole or trench big enough for each object, then carefully burying the object so as to disturb only a minimum amount of sand. The sand was packed and shaped around the object in order to maximize the coupling of the sediment to the object. The objects were buried to a depth as to allow the top of the object to remain flush with the sediment surface. This was done in order to maximize the interaction of the surface waves with buried objects and to mimic the actual emplacement of real land mines. For some experiments, an additional technique was employed to further maximize the coupling of the buried object with the sediment. For these experiments, both the powder keg and the cylinder were first buried, using normal procedures, then were left at the beach test site for several days. The buried objects were washed over by the tides several times. Consequently, the coupling with the sediment was the best possible that could be achieved. An interesting note was that the mines were found to be at a different depth in the sand than when they were emplaced. Either by the natural scouring action of the tides, or by new sand being deposited over the objects, they had three to four inches of sand covering them when detection experiments commenced. Two examples of the buried objects, with their end caps removed to facilitate weight addition, are shown in Figures 3.12 and 3.13.

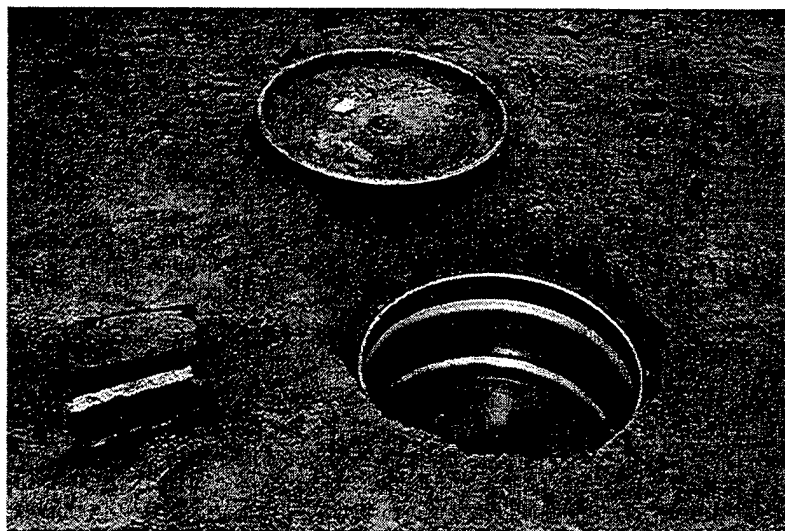


Figure 3.12. Buried powder keg target with top removed.



Figure 3.13. Buried cylinder with end cap removed.

3. Summary

Examples of the collected data plots and imaginary crossed power plots have been presented to show how these signals are used for detection of the buried targets. The strengths of the received target reflections, coupled with propagation losses due to signal attenuation and spreading, will provide the target-strength measurements of the buried objects. The next chapter presents the results of several successful target detections and also computes the target strengths of the targets.

(This page intentionally blank)

IV. TARGET DETECTION AND TARGET-STRENGTH MEASUREMENTS

Using the signal processing techniques described in the previous chapter, the following sections describe the qualitative and quantitative experimental results from several target detection experiments. The following section will detail the procedures used for the estimation of target strengths and propagation losses due to cylindrical spreading and absorption. A subsequent section will compare and analyze target-strength measurements observed among the different experiments. As a reminder, each target detection and target-strength measurement was achieved on a separate day, with varying conditions (frequencies, wavespeeds, and targets), and is considered a separate experiment. However, relative comparisons can be made, given the consistency of the procedures and methods utilized.

The following section will provide imaginary crossed power plots produced from target detection data. As previously discussed, the 8-channel plots of the received signals (two tri-axial seismometers and two uni-axial accelerometers) provide little, if any, indication of a target reflection. Other than for the example in Chapter III, there is no necessity to include each of those plots respective to a target detection. Since the imaginary crossed power plots provide the evidence of target detection in this research, they are exhibited for all significant detections. Data from these plots will also provide measurements of target strengths. Following an overview of the successful detections, some comparisons of target strengths will be discussed.

A. CALCULATIONS OF TARGET STRENGTHS

In the realm of underwater sound, a calculation used with active sonar, *target strength*, refers to the reflection, or echo, returned from an underwater target. With regard to the sonar equation, target strength is defined as 10 times the logarithm to the base 10 of the ratio of the intensity of the sound returned by the target in some direction, at a distance of 1 m from its "acoustic center," to the incident intensity from a distant source, and is given by

$$TS \equiv 10 \log \left. \frac{I_r}{I_i} \right|_{r=1} \text{ dB}, \quad (4.1)$$

where I_r = intensity of return at 1 m and I_i = incident intensity [Ref. 16]. An example of how target strengths are calculated here from the imaginary crossed power follows, using actual data from a target detection.

Referring to Figure 3.11, the source-receiver distance was 10 ft (3 m) and the receiver-target distance was 6 ft (2 m) on this particular experimental day. Figures 4.1 and 4.2 show the imaginary power versus time, converted to range, obtained from the average of a sequence of target detection experiments, employing a single cycle pulse. Figure 4.1 shows the amplitude of the imaginary power from 0 to 30 ft (0 to 10 m), and clearly exhibits the incident wave signal as it passes the seismometer receivers at a range of 10 ft (3 m) from the source. Figure 4.2 shows the amplitude of the imaginary power for ranges of approximately 23 ft (7 m). The actual source-target-receiver distance in this experiment was 22 ft (7 m).

The intensities used in (4.1) were estimated from data obtained from Figures 4.1 and 4.2 as follows. First, the incident intensity at the receiver was estimated from Figure 4.1. It was estimated as the peak value of the imaginary crossed power observed during the time the incident wave passed by the receiver. For this example, using receiver #1, this value is 0.7, at a range of 10 ft (3 m). Next, the return intensity, at the location of the same receiver, was estimated. From Figure 4.2, this value is 0.024, at a (round trip) range of 23 ft (7 m). These were corrected for attenuation, to provide estimates of I_i and I_r in (4.1), as follows.

Attenuation experiments were conducted to provide an estimation of signal attenuation at the beach test site. Using the "standard" equipment set-up, the seismometers were placed at regular intervals from 10 to 70 ft (3 to 22 m). A plot of that data, in imaginary power versus range is shown in Figure 4.3. In this particular case, attenuation can be estimated very nearly as cylindrical spreading ($1/R$ dependence) at the ranges being used in these experiments, up to 15 ft (3 m). Therefore, a correction for cylindrical spreading was applied to the incident and returned wave intensity values

estimated from Figures 4.1 and 4.2, in order to estimate the values of I_i and I_r in (4.1). For this example, the receiver and target ranges from the source are 10 ft (3 m) and 16 ft (5 m), respectively. The estimated value of I_i is therefore 10/16 (-2.2 dB) times the estimated value of the incident intensity at the receiver. The range from the target to the receiver is 6 ft (2 m) for this example. Then, the estimated value of I_r at a range of 1 m is $\frac{1}{2}$ (-3 dB) times the estimated value of the returned intensity at the location of the receiver. From (4.1), then, the estimated target strength in this example is -9.45 dB. All target strengths were estimated in this manner.

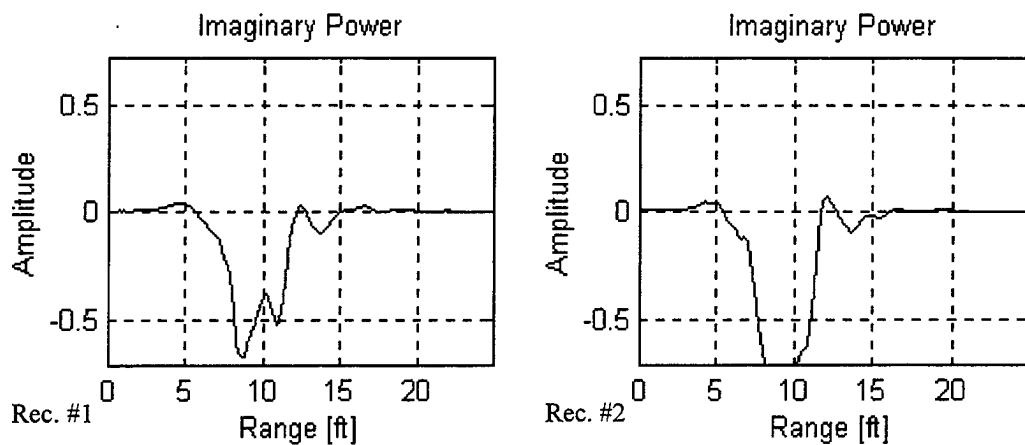


Figure 4.1. Imaginary power plot for incident wave.

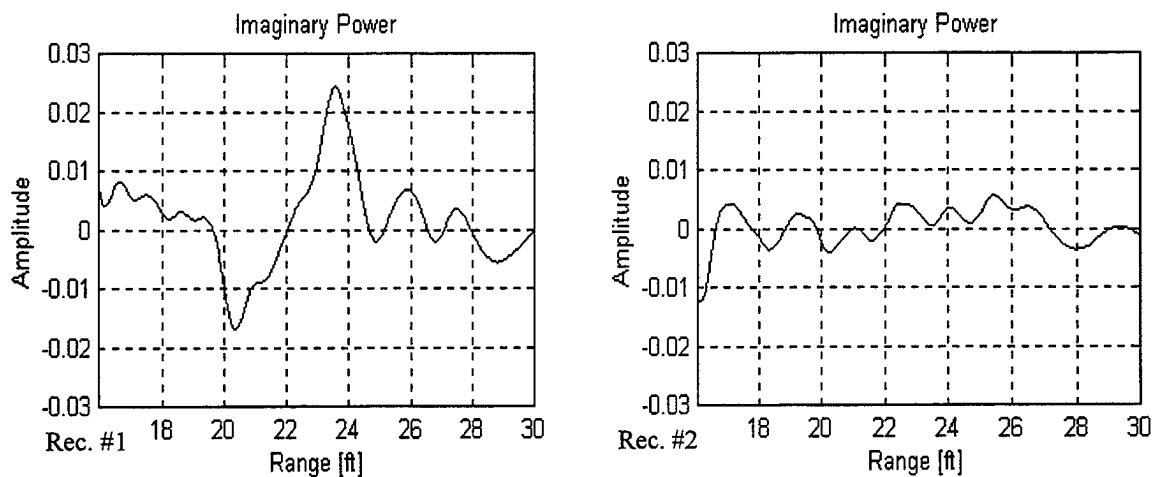


Figure 4.2. Imaginary power lot for the reflected signal.

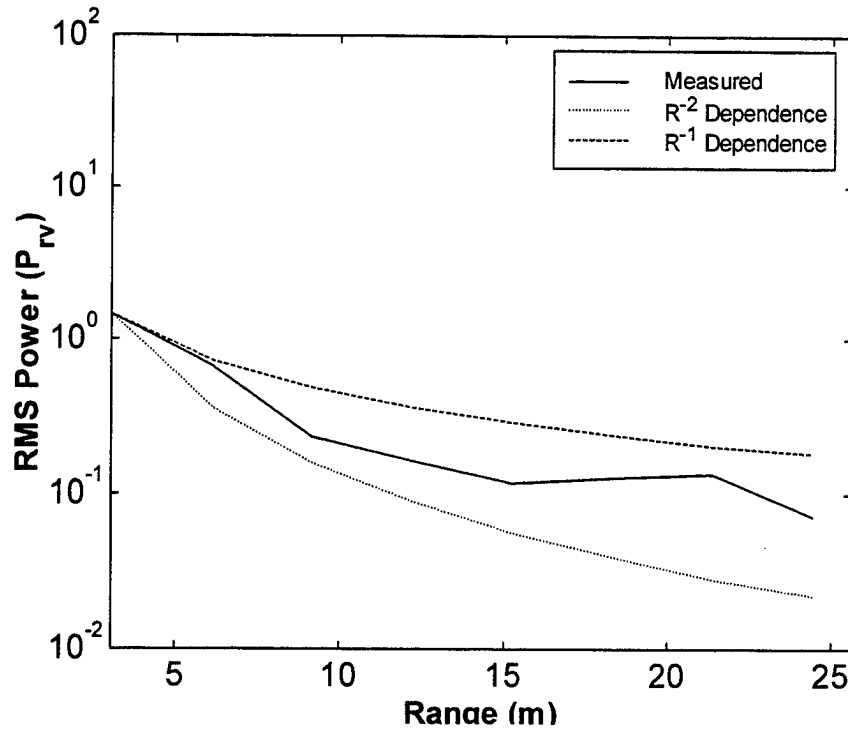


Figure 4.3. Plot of attenuation at beach test site.

B. TARGET DETECTIONS AND TARGET-STRENGTH MEASUREMENTS

The following significant target detections will each be presented in a separate section. Details of the equipment configuration will be provided, referenced to Figure 3.11, with any variances in distances (source-receiver and source-target) noted. Also provided for each experiment will be the frequency, wavespeed, and type of target being used. For the first three experiments (October 16th, 20th, and 23rd), the targets, the gas cylinder in each case, were buried just a few hours prior to data collection. For the latter two experiments (November 6th and 10th), the targets (cylinder and powder keg) were left buried for several days prior to data collection. The data illustrate the variation in scattering strength with target weight. In the three latter experiments (October 23rd, November 6th and 10th) lead weights were incrementally added to the target. Target strengths will be estimated for each experiment and for those experiments where various weights were used. Plots of target strength versus weight are provided. The detections will be referred to by the date on which the experiments were conducted.

1. Empty Gas Cylinder, October 16th 1998

The first successful detection of a target in this thesis work, the gas cylinder in this case, occurred on October 16th. It was uncertain at the time whether the target had been detected, but only after subsequent unambiguous detections, using similar procedures, was this detection confirmed. Using the procedures described in Chapter III, the optimum frequency and corresponding wavespeed were determined as 90 Hz and 260 ft/s (79 m/s), respectively. The seismometers were located 2 ft (0.6 m) from the sources and the target was located 10 ft (3 m) from the sources. The source-target-receiver distance was 18 ft (5.5 m). The target was empty and weighed 150 lbs (68 kg). The imaginary crossed power plots are provided in Figures 4.4 and 4.5, respectively.

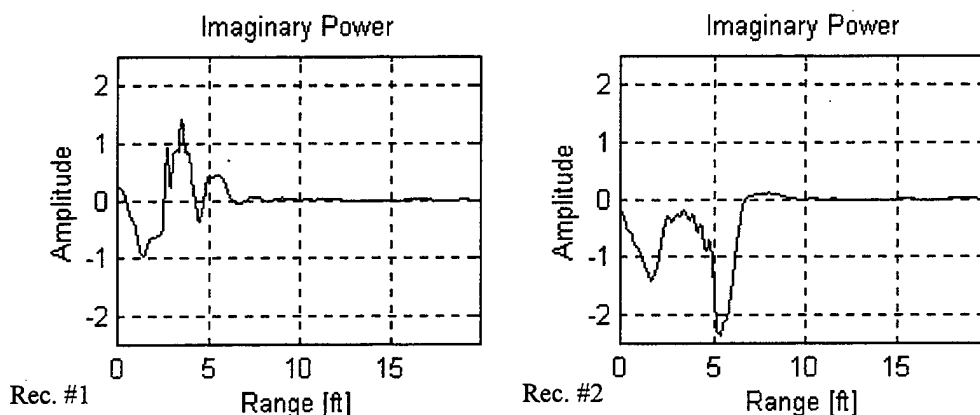


Figure 4.4. Imaginary power plot for incident wave, October 16th.

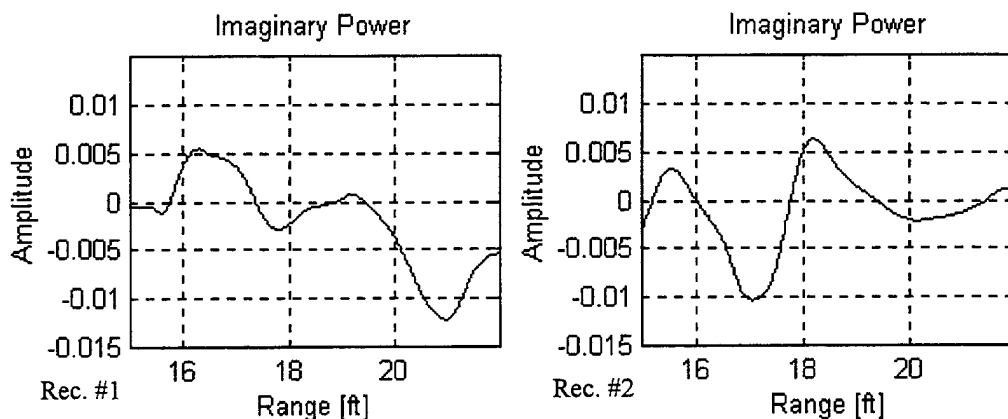


Figure 4.5. Imaginary Power Plot for scattered wave from cylinder, October 16th.

The signal passing the receiver can be seen at a distance of 2 ft (0.6 m) in Figure 4.4. In Figure 4.5, the target can be seen at 17 ft (5.2 m) for receiver #2. The computed target strength, using the procedures from above, is -9.10 dB.

2. Empty Gas Cylinder , October 20th 1998

For this subsequent detection of the target, the empty cylinder was again used. The optimum frequency and corresponding wavespeed were determined as 90 Hz and 226 ft/s (68 m/s), respectively. The seismometers were located 6 ft (3 m) from the sources and the target was located 13 ft (3.9 m) from the sources. The source-target-receiver distance was 20 ft (6 m). The target was again empty and weighed 150 lbs (68 kg). The imaginary crossed power plots for the total range and for the range where the target should be found are provided in Figures 4.6 and 4.7, respectively.

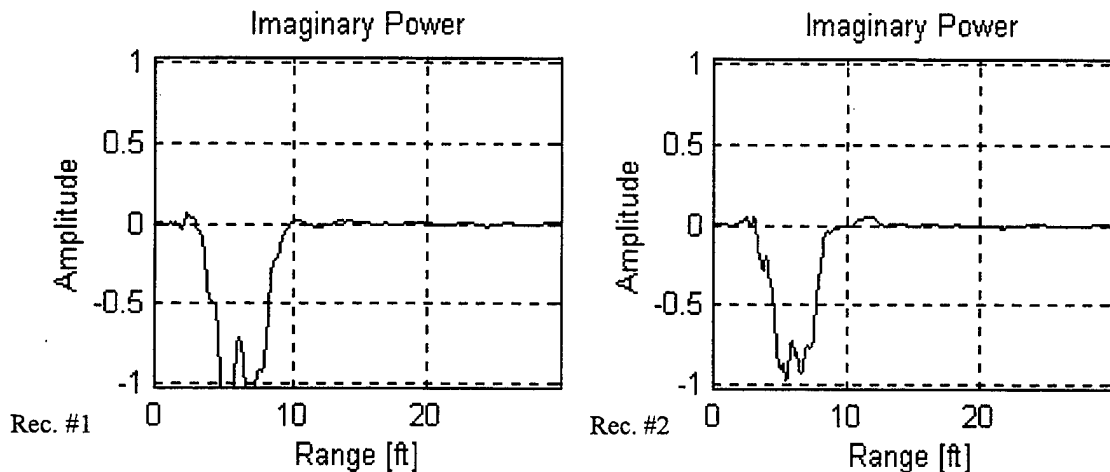


Figure 4.6. Imaginary power plot for incident wave, October 20th, 1998.

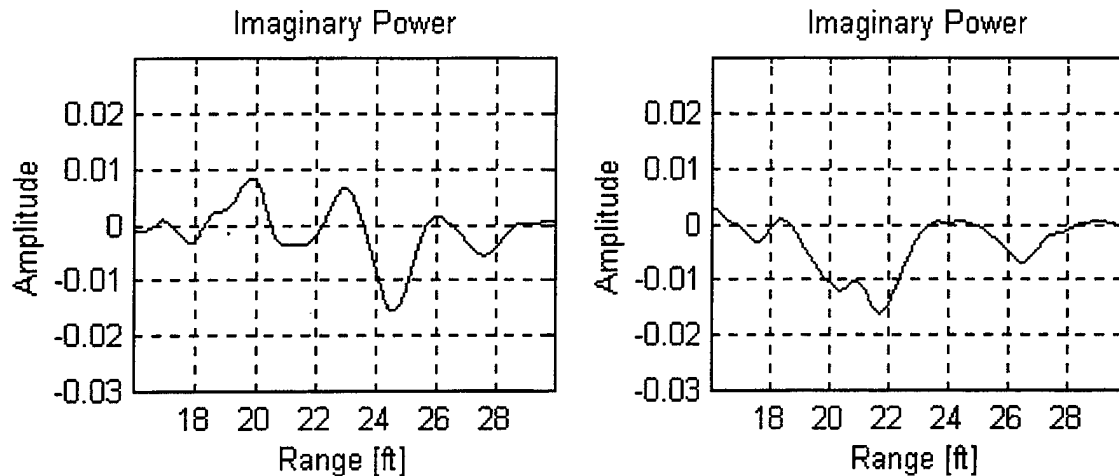


Figure 4.7. Imaginary power plot for scattered wave from cylinder, for October 20th.

The signal passing the receiver can be seen at a distance of 6 ft (2 m) in Figure 4.6. In Figure 4.7, the target can be seen at 22 ft (6.6 m) for receiver #2. The computed target strength, using the procedures from above, is -11.20 dB.

3. Gas Cylinder, October 23rd 1998

For this experiment, the equipment configuration and distances were similar to those used on October 20th. For this detection of the target, the empty cylinder and the cylinder filled with 18 lead blocks were used. The weight of the empty cylinder was 150 lbs (68 kg) and with the lead blocks it weighed 618 lbs (280 kg), a factor of four difference. The optimum frequency and corresponding wavespeed were determined as 70 Hz and 220 ft/s (67 m/s), respectively. The seismometers were located 6 ft (2 m) from the sources and the target was located 11 ft (3.3 m) from the sources. The source-target-receiver distance was 16 ft (6 m). The imaginary crossed power plots for the total range and for the range where the target should be found are provided in Figures 4.8 and 4.9, respectively. Here, several plots are presented in the figures. The first is the background signal, or "back", which has no target present. The second is the empty cylinder, or "TGT", and the third is the target with the weight added, or "heavy."

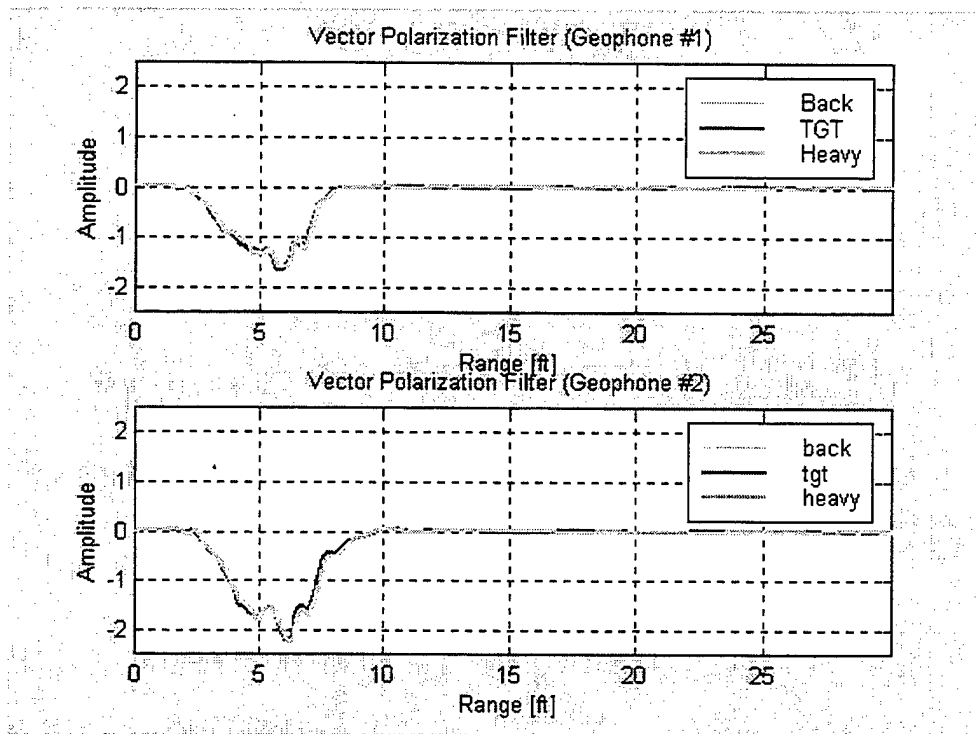


Figure 4.8. Imaginary power plot for cylinder, October 23rd with three data plots.

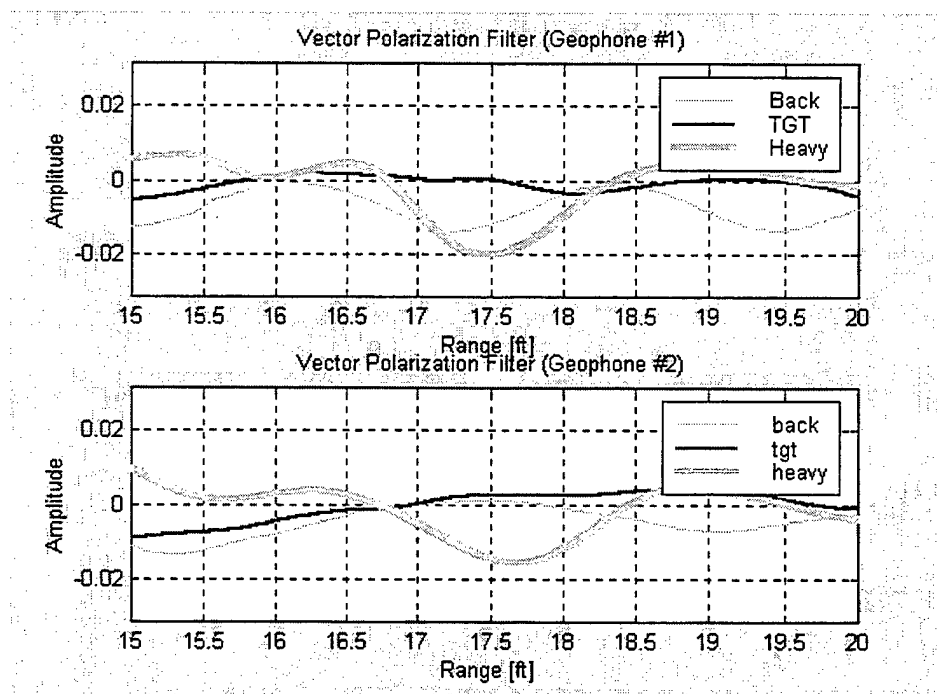


Figure 4.9. Imaginary power plot for cylinder, October 23rd with three data plots.

The incident signal can be seen at a distance of 6 ft (2 m) in Figure 4.8, and is identical for each weight. In Figure 4.9, the loaded target can be seen at 17.5 ft (5.3 m) for receiver #1 (Geophone #1). The computed target strength is -13.90 dB. The signal for the empty cylinder is indistinguishable in the plot.

4. Gas Cylinder, November 6th 1998

For this experiment, the equipment configuration and distances were similar to those used previously. For this detection of the target, the cylinder was initially empty, weighing 150 lbs (68 kg), and it was then incrementally filled with lead blocks up to 16 blocks, in groups of four, for a maximum weight of 566 lbs (257 kg), a factor of four difference. The cylinder was buried for 4 days prior to data collection. The optimum frequency and corresponding wavespeed were determined as 80 Hz and 295 ft/s (89 m/s), respectively. The seismometers were located 10 ft (3 m) from the sources and the target was located 16 ft (4.8 m) from the sources. The source-target-receiver distance was 22 ft (6.7 m). The imaginary crossed power plots are provided in Figures 4.10 and 4.11, respectively. Here, several plots are presented in the figures. The first is the empty cylinder, or "150lbs", and so on for each weight increment added.

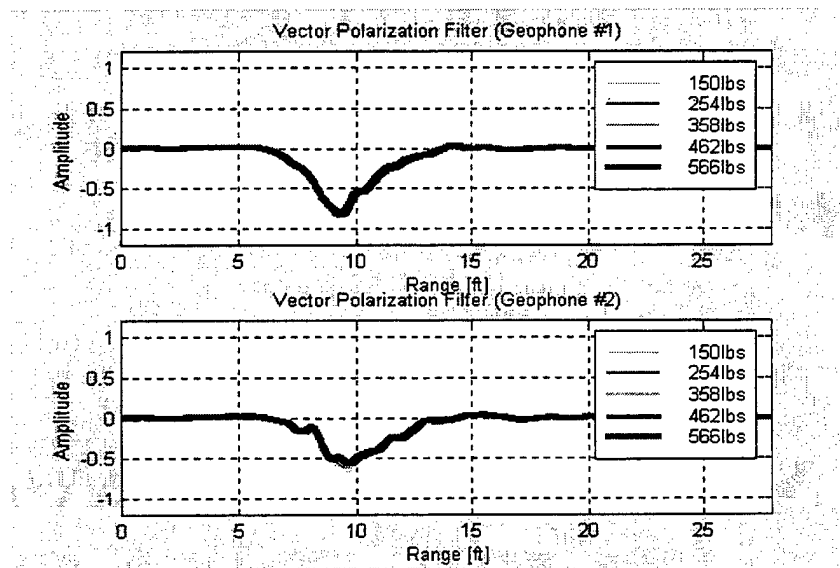


Figure 4.10. Imaginary power plot for cylinder, November 6th with five data plots.

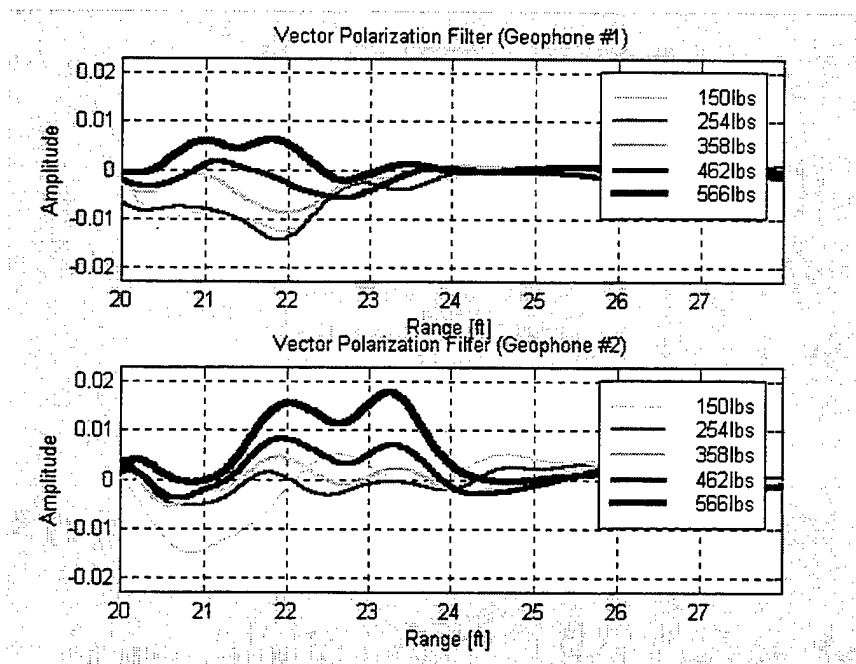


Figure 4.11. Imaginary power plot for cylinder, November 6th with five data plots.

The signal passing the receiver can be seen at a distance of 10 ft (3 m) in Figure 4.10, and the signal is essentially the same for each weight loading, despite the time differential for each record (approximately 5 minutes). In Figure 4.11, the target can be seen at various amplitudes at 22 ft (6.7 m) for receiver #2 (Geophone #2). The computed target strengths for the various weights are given in Table 1.

Cylinder Mass lbs (kg)	Target Strength (dB)
150 (68)	No signal detected
254 (115)	-20.40
358 (162)	-16.42
462 (210)	-13.87
566 (257)	-11.65

Table 1. Cylinder weights with respective target strengths.

5. Powder Keg, November 10th 1998

For this experiment, the equipment configuration and distances were similar to those used previously. The powder keg was used as the target in this experiment. The powder keg was buried for 8 days prior to the experiment day. During this time, it was subjected to several tidal cycles and under water for brief periods of time. Weight addition procedures were similar to those used on November 6th, 4 blocks initially, up a maximum of 24. The weight of the empty powder keg was 16 lbs (7 kg) and the total weight, with the lead blocks, increased from 120 lbs (54 kg) to 640 lbs (290 kg), a factor of five difference. The optimum frequency and corresponding wavespeed were determined as 80 Hz and 270 ft/s (82 m/s), respectively. The seismometers were located 10 ft (3 m) from the sources and the target was located 16 ft (4.8 m) from the sources. The source-target-receiver distance was 22 ft (6.7 m). The imaginary crossed power plots for the total range and for the range where the target should be found are provided in Figures 4.12 and 4.13, respectively. Here, several plots are presented in the figures. The first is the powder keg with 4 blocks, or "120lbs", and so on for each weight increment added.

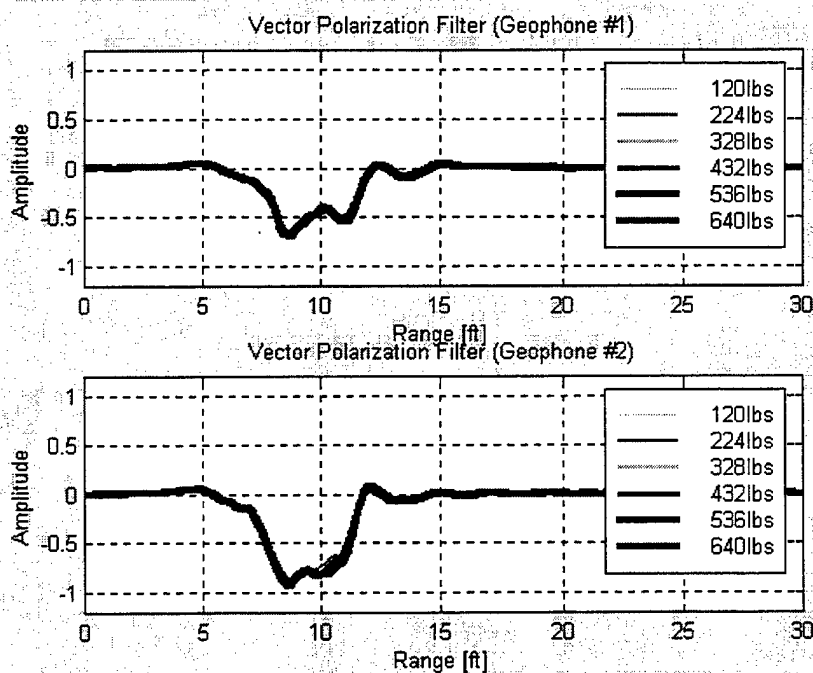


Figure 4.12. Imaginary power plot for powder keg, November 10th with six data plots.

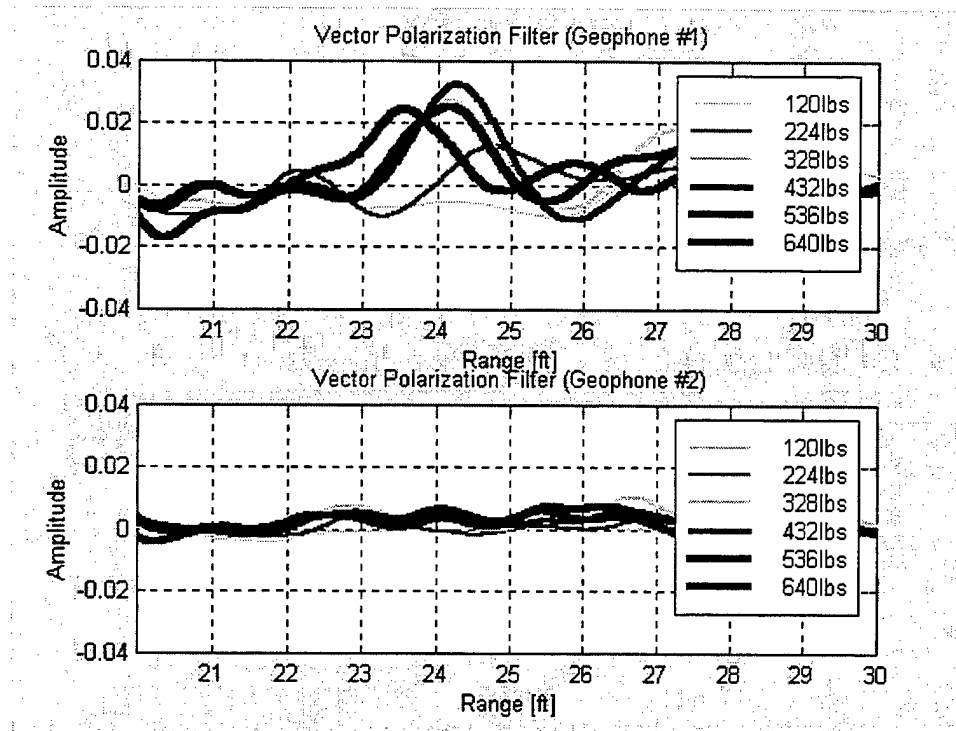


Figure 4.13. Imaginary power plot for powder keg, November 10th with six data plots.

The signal passing the receiver can be seen at a distance of 10 ft (3 m) in Figure 4.12, and, again, the signals are essentially the same for each weight. In Figure 4.13, the target can be seen at various amplitudes at 24 ft (7.3 m) for receiver #1 (Geophone #1). The computed target strengths for the various weights are given in Table 2, using peak values. The source for the variation in peak values is unknown.

Powder Keg Mass lbs (kg)	Target Strength (dB)
120 (54)	No signal detected
224 (102)	-13.41
328 (149)	-9.61
432 (196)	-9.26
536 (243)	-9.61
640 (290)	-9.79

Table 2. Powder keg weights with respective target strengths.

C. OBSERVATIONS AND SUMMARY

Analysis of the results from the target detection measurements yields several interesting points. As was previously mentioned, using vector polarization filtering (crossed power), the location of maximum deflection of the imaginary crossed-power plot, positive or negative from zero amplitude, was used to estimate the receiver and target locations. For the majority of the experiments, the deflection in the crossed power plot, caused by the passing of the incident wave at the receiver, yielded a source-receiver distance, which is in close agreement with the actual distance. However, the round trip target distance estimated using the reflected wave may be observed as much as 2 ft (0.67 m), or 10%, closer or farther away than the actual target location. Another point regarding location accuracy is that a particular seismometer may not receive the same signal as an adjacent receiver separated a lateral distance of only 4 ft (1.2 m), equidistant from both the sources and the target. The data provided by each receiver, as observed in many of the preceding plots, was somewhat similar, but rarely identical. Many underlying causes might have contributed to these inconsistencies. Further research must explore these factors.

As mentioned, the positive or negative deflection in the imaginary crossed power plot also determines whether the received signal is traveling in a prograde or retrograde elliptical orbit. For the first three experiments, October 16th, 20th, and 23rd, the incident signal has a negative deflection as it passes the receiver with the seismometers' positive x-axis oriented away from the sources. However, this incident signal is a prograde wave, due to the directivity of the seismometer (see Section III.D.2, Figure 3.11), which is "pointing" away from the source (Figures 4.4, 4.6, and 4.8), causing an inversion of the polarity. The scattered signal also has a negative deflection, but this indicates a retrograde wave (Figures 4.5, 4.7, and 4.9), since the receiver is now "pointing" at target. For these three experiments, the incident wave has a prograde motion and the reflected wave has a retrograde motion. In contrast, the reflected signals from the targets for the November 6th and 10th experiments had positive deflections, indicating prograde motion (Figures 4.11, 4.13). The incident signals for these two experiments were prograde waves, just as in the first three experiments. However, the deflection of the imaginary

power was positive for the received signals, opposite of the generated signal passing by the receiver. For these last two experiments, the incident and reflected signals had similar elliptical rotations, which differed from earlier experiments where the incident signals had prograde motion and the reflected waves had retrograde motion.

Rayleigh waves are unique, in that they travel in two different elliptical motions within a depth equal to their wavelength. Rayleigh waves travel in a retrograde orbit at the interface, but change to a prograde orbit at a depth equal to a fraction (around 0.1λ to 0.2λ) of their wavelength, this being dependent upon frequency. The wavelengths used in all of the experiments were at most 3 ft (1 m), with most being around 2.4 to 2.7 ft (0.8 to 0.9 m). In the first three experiments, the targets (cylinder) were buried with the top surface protruding slightly from the sand, leaving 6 to 7 in (15 to 18 cm) under the surface. These targets were buried only for a few hours prior to data collection. In these cases the target would reside in the wavelength fraction where retrograde Rayleigh waves propagate. For the last two experiments, the targets (power keg and cylinder) were covered by several inches of sand (see Figures 3.12 and 3.13) and the bulk of the objects were in the prograde region. These targets were buried several days prior data collection, subjected to the tidal cycle during this period. The reason for the polarities of the reflected signals recorded is unknown. Further research is highly recommended to fully investigate this point.

The comparison of target strengths yielded several general observations. Because of the varying optimum frequency and corresponding wavespeed, in which sediment properties played a large role, it is difficult to make direct comparisons. Table 3 summarizes the experiments, test parameters, incident and reflected wave motion, and associated target strengths. Figures 4.14 and 4.15 are plots of the November 6th and 10th target-strength data and associated target weights. The target-strength measurements for the cylinder are comparable, given consideration to the use of different frequencies, wavespeeds, and target distances. Figure 4.14 indicates that, for the cylinder, as more weight is added the target strength increases. However, for the powder keg, the target strength increases to a point with weight addition, but as more weight is added, the target strength levels off.

Date	Freq. (Hz)	Wavespeed ft/s (m/s)	Tgt Dist. ft. (m)	Target	Target Mass lbs (kg)	Inci. Wave	Refl. Wave	TS dB
Oct 16 th	90	260 (79)	18 (5.5)	Cylinder	150 (68)	Pro	Retro	-9.10
Oct 20 th	90	226 (68)	20 (6.1)	Cylinder	150 (68)	Pro	Retro	-11.20
Oct 23 rd	70	220 (67)	16 (4.8)	Cylinder	618 (280)	Pro	Retro	-13.90
Nov 6 th	80	295 (89)	22 (6.7)	Cylinder	150 (68)	Pro	Pro	n/a
Note 1	"	"	"	"	254 (115)	"	"	-20.40
	"	"	"	"	358 (162)	"	"	-16.42
	"	"	"	"	462 (209)	"	"	-13.87
	"	"	"	"	566 (257)	"	"	-11.65
Nov 10 th	80	270 (82)	22 (6.7)	Powder Keg	120 (54)	Pro	Pro	n/a
Note 1	"	"	"	"	224 (102)	"	"	-13.41
	"	"	"	"	328 (149)	"	"	-9.61
	"	"	"	"	432 (196)	"	"	-9.26
	"	"	"	"	536 (243)	"	"	-9.61
	"	"	"	"	640 (290)	"	"	-9.79

Note 1: The targets in these two experiments were buried for an extended period of time, resting much deeper in the sediment than the targets in the first three experiments

Table 3. Summary of target detections and target strengths

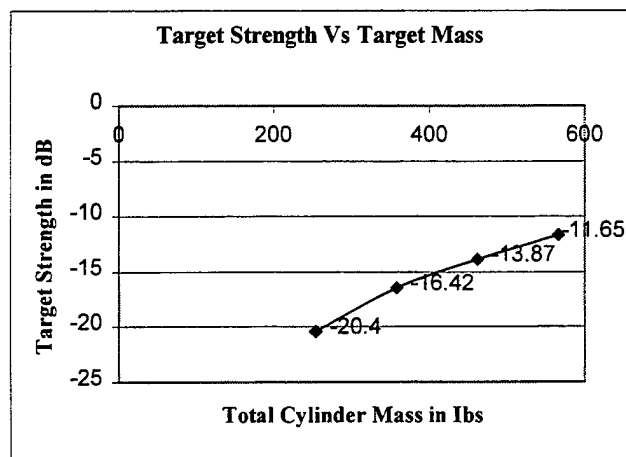


Figure 4.14. Target strength vs. target mass for cylinder target.

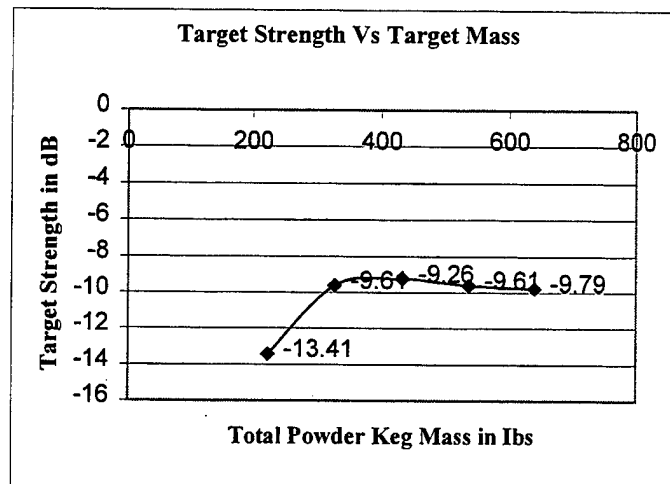


Figure 4.15. Target strength vs. target mass for powder keg target.

Target detection and the calculation of target strengths are very difficult experimental events. Despite the great effort to ensure procedures were consistent across all the experiments, there was a degree of inherent variability. For example, the optimum frequency, corresponding wavespeed, and accuracy of detection distances varied from experiment to experiment. Environmental conditions (reflection, refraction, sand density and moisture content) probably contributed a degree of inconsistency across all experiments. However, given the range of experiment variables encountered, target-strength values are consistent throughout all of the experiments. While little research has been conducted in using a seismo-acoustic sonar to detect buried objects, and also in the calculation of seismo-acoustic surface wave target strength, the results of this research are highly promising and should be continued. In the following chapter, some brief conclusions will be drawn concerning this thesis research.

V. CONCLUSIONS

The concept of a seismo-acoustic sonar to detect mine-like objects buried in the beach and surf zone environments was demonstrated successfully, as detailed in this thesis work. These successful experiments required the identification and recording of the reflection of a buried object insonified by seismic interface waves. The target reflection was then processed to determine target position. The detection of these buried objects, using vector polarization filtering, without the prior utilized method of background subtraction, is a significant accomplishment. The potential application of this concept in military operations requiring mine countermeasures is encouraging. However, much further research and development is needed to refine and optimize equipment and signal processing techniques to even begin to approach the fielding of a system capable of capitalizing on this concept. The key signal processing techniques used in this present work, specifically vector polarization filtering, were crucial to successful target detection and target-strength measurement.

The target-strength measurements proved to be in relatively consistent agreement across the multitude of experiments conducted. These measurements were highly dependent upon distance (source-target-receiver) and target size and mass. Target objects, smaller than the objects (cylinder and powder keg) used in this research, simply were not detectable with the present research tools. The addition of mass to the detected objects greatly improved detection efforts. Also, special care was taken to improve coupling of the sediment with the buried object in each experiment. The use of more sources and sensors, in arrays, should be expected to increase the research tool's ability to detect lighter targets in future experiments.

Relevant target strengths were measured and calculated for each target detection. These target strengths were calculated by application of the sonar equation and an associated target strength equation. Based on the success events of this research, the development of a suitable seismo-acoustic sonar, the detection of buried objects, and calculations of buried object target strengths, further research and development of this concept is warranted and should be vigorously pursued.

(This page intentionally blank)

LIST OF REFERENCES

1. TenCate, J.A., Muir, T.G., Caiti, A., Kristensen, A., Manning, J.F., Shooter, J.A., Koch, R.A., Michelozzi, E., "Beamforming on Seismic Interface Waves with an Array of Geophones on the Shallow Sea Floor," *IEEE Journal of Oceanic Engineering*, vol. 20, (4), Oct. 1995.
2. Smith, E., Wilson, P.S., Bacon, F.W., Manning, J.F., Behrens, J.A., Muir, T.G., "Measurement and Localization of Interface Wave Reflections from a Buried Target," *Journal Acoustical Society of America*, vol. 103 (5), May 1998.
3. Smith, E., "Scattering of Interface Waves from Pointlike Obstacles," *Journal Acoustical Society of America*, vol. 103 (5), May 1998.
4. Gaghan, Jr., F.E., *Discrete-Mode Source Development and Testing for New Seismo-Acoustic Sonar*, Master's Thesis, Naval Postgraduate School, Monterey, CA, Mar. 1998.
5. U.S. Department of State, Bureau of Political Military Affairs, *Hidden Killers: The Global Landmine Crisis*, Washington, DC, Dec. 1994.
6. U.S. Navy, Naval Doctrine Command, "Concept for Future Naval Mine Countermeasures in Littoral Power Projection," Washington, DC, May 1998.
7. National Research Council, Naval Studies Board, "Technology for the United States Navy and Marine Corps, 2000-2035," vol. 7, Undersea Warfare, Washington, DC, 1997.
8. Muir, T.G., Smith, D.E., Wilson, P.S., "Seismo-Acoustic Sonar for Buried Object Detection," Proceedings of the Symposium, *Technology and the Mine Problem*, Naval Postgraduate School, Monterey, CA, Nov. 1996.
9. Stewart, W.F., *Buried Object Detection Using Surface Waves*, Master's Thesis, Naval Postgraduate School, Monterey, CA, Sep. 1995.
10. Toderoff, D., Editor, *Naval Research Reviews*, vol. 49 (3), 1997.
11. Lim, R., Lopes, J., Hackman, R., Todoroff, D., "Scattering by Objects Buried in Underwater Sediments: Theory and Experiment," *Journal Acoustical Society of America*, vol. 93 (4), Apr. 1993.
12. Lim, R., "Scattering by an Obstacle in a Plane-Stratified Poroelastic Medium: Application to an Obstacle in Ocean Sediments," *Journal Acoustical Society of America*, vol. 95 (3), Mar. 1994.

13. Au, W.W.L., Shizumura, R.H., Moons, J., Roitblat, H.L., Hicks, R.C., "Sonar Detection and Classification of Buried Targets Using Broadband Dolphin-like Signals," *Journal Acoustical Society of America*, vol. 104 (3), Sep. 1998.
14. Fitzpatrick, S.M., *Source Development and Testing of a Seismo-Acoustic Sonar*, Master's Thesis, Naval Postgraduate School, Monterey, CA, Dec. 1998.
15. U.S. Navy, Office of the Chief of Naval Operations, Director of Expeditionary Warfare, *United States Naval Mine Warfare Plan*, 3d Edition, FY 96-97, Washington, DC, 1995.
16. Urick, R.J., *Principles of Underwater Sound for Engineers*, McGraw-Hill, Inc., 1967.

INITIAL DISTRIBUTION LIST

1. Defense Technical Information Center.....2
8725 John J. Kingman Rd., STE 0944
Ft. Belvoir, Virginia 22060-6218
2. Dudley Knox Library2
Naval Postgraduate School
411 Dyer Rd.
Monterey, California 93943-5101
3. Dr. Douglas Toderoff.....2
Office of Naval Research, Code 321
800 N. Quincy St.
Arlington, Virginia 22217-5660
4. Director, Training and Education.....1
MCCDC, Code C46
1019 Elliot Rd.
Quantico, Virginia 22134-5027
5. Director, Marine Corps Research Center.....2
MCCDC, Code C40RC
2040 Broadway Street.
Quantico, Virginia 22134-5107
6. Director, Studies and Analysis Division.....1
MCCDC, Code C45
300 Russell Road
Quantico, Virginia 22134-5130
7. Dr. Jeffrey Simmen.....1
Office of Naval Research, Code 3210A
800 N. Quincy St.
Arlington, Virginia 22217-5660
8. Dr. Raymond Lim.....1
Coastal Systems Station, Code R22
6703 W. Highway 98
Panama City, Florida 32407-7001
9. Dr. David Skinner.....1
Coastal Systems Station
6703 W. Highway 98
Panama City, Florida 32407-7001

10. Library, Coastal Systems Station.....	1
6703 W. Highway 98	
Panama City, Florida 32407-70001	
11. Professor Steven R. Baker, Code PH/Ba.....	2
Department of Physics	
Naval Postgraduate School	
Monterey, California 93943-5000	
12. Professor Thomas G. Muir, Code PH/Mt.....	2
Department of Physics	
Naval Postgraduate School	
Monterey, California 93943-5000	
13. Major Patrick W. Hall.....	1
3211 Titanic Drive	
Stafford, Virginia 22554-2628	
14. Dr. Nickolas P. Chotiros.....	1
Applied Research Laboratories	
University of Texas at Austin	
P.O. Box 8029	
Austin, Texas 78713-8029	
15. Dr. Michael Pestorius.....	1
Applied Research Laboratories	
University of Texas at Austin	
P.O. Box 8029	
Austin, Texas 78713-8029	
16. Library.....	1
Applied Research Laboratories	
University of Texas at Austin	
P.O. Box 8029	
Austin, Texas 78713-8029	
17. Dr. Peter Rogers.....	1
School of Mechanical Engineering	
Georgia Institute of Technology	
Atlanta, Georgia 30332	
18. Dr. Peter Krumhansel.....	1
Bolt, Beranek, & Newman, Inc.	
Union Station	
New London, Connecticut 06320	